Spring 2020

GENETIC REMOVAL OF TOXIN AND INTEGRASE GENES FROM A STAPHYLOCOCCAL BACTERIOPHAGE

Hannah Sparks

GENETIC REMOVAL OF TOXIN AND INTEGRASE GENES FROM A

STAPHYLOCOCCAL BACTERIOPHAGE

by

Hannah Sparks

A thesis submitted in partial fulfillment of the

requirements for the degree of

Interdisciplinary Master of Science

Montana Tech

2020

Abstract

Bacteriophages, or phages, are viruses that specifically infect and kill bacterial cells. Phages are the most numerous biological entities on Earth, with an estimated population size of 10^{31} (1). Discovery, purification, and characterization of phages illuminate the composition of the microbial world and provide potential applications in medicine. To combat antibiotic-resistant bacteria, phages are being investigated as supplements or alternatives to antibiotics. Methicillin-resistant *Staphylococcus aureus* (MRSA) is a commonly acquired infection in hospitals that has become difficult to treat due to its resistance to antibiotics commonly used to treat ordinary *S. aureus* infections (20). Bacteriophage, JB, isolated from dairy cow hair samples by Tyler Nygaard at Montana State University, has the ability to infect MRSA USA300 strain LAC. Genome annotation of this phage characterized it as a 42,683 bp circularly permuted genome with 68 putative protein coding genes, and a G/C content of 35.2%. Through bioinformatic analysis it was discovered that in a cluster of reverse transcribed (genes 30-33), putative integrase and toxin genes were present (21). In order for this phage to be used therapeutically in mammalian organisms, the deletion of these genes is essential to prevent the possibility for the phage to produce viable lysogen bacterial cells with enhanced pathogenicity. Genetic engineering to remove genes 30-33 was performed using type the type II CRISPR-Cas9 system to generate a strictly lytic deletion mutant JB bacteriophage, JBΔ30-33. The creation of the lytic derivative of JB bacteriophage, JBΔ30-33, was confirmed by clear plaque morphology, polymerase chain reaction, and DNA sequencing.

Dedication

I would like to thank my parents, Heather and André, as well as my stepparents, Dave and Megan. Each of them has shaped me into the person that I am today and have contributed to my eagerness to keep learning, growing, and humbling myself.

I would also like to also thank my fiancé, A.J. Robinson, for continually encouraging me to keep moving forward to pursue whatever degree or goal I choose. A.J. has always fit his life into mine and has been willing to adapt so that I can achieve the career that I want.

Finally, I am thankful for the life that God has provided me and for my ability to get an education. There are a lot of people in the world who are unable to receive an education, much less one at a graduate level; therefore, I am grateful for the education I have received.

Acknowledgements

With the highest regard, I would like to thank Montana Technological University's Biological Sciences Department for their constant support and dedication to my education. The faculty in the Biology Department have fostered my true love for molecular biology and research. I would like to specifically thank Dr. Marisa Pedulla for her continual dedication to me as a mentor. Dr. Pedulla has developed me into a professional who can thrive in educational, and work environments and she has provided me with opportunities to grow in my career. More importantly, she taught me through her own actions that compassion for others is just as important as any scientific discovery.

My research was made possible through the support of my committee members, Drs. Joel Graff, Katie Hailer, Jessica Gregory, and Julie Hart. The members of my committee were always willing to help me think through the hardest obstacles of my project as well as provide valuable insight from their personal experiences in research. Without the help of my brilliant committee members, my project would not have been possible.

Table of Contents

List of Figures

Glossary of Terms

Term	Definition
Bacteriophage	A virus that infects and kills bacteria.
Lysogen	A bacterium harboring a bacteriophage genome within the bacterial chromosome.
CRISPR-Cas9	A protein/RNA complex that creates double stranded breaks within a DNA sequence of interest.
Toxin	A small molecule, peptide, or protein that is toxic when introduced to body tissues by interaction with cellular receptors or enzymes.
Bacteriophage Integrase	A site-specific recombinase that inserts a bacteriophage genome into a bacterial chromosome.
Antibiotic Resistance	Bacteria or other microorganisms' that are resistant to antibiotic treatment.

1. Background

1.1. Bacteriophages

Bacteriophages, or phages, are viruses that specifically infect and kill bacterial cells. Phages are the most numerous biological entities on Earth, with an estimated population size of 10^{31} (1). Phages were co-discovered by William Twort in 1915 and Felix d'Herelle in 1917 (2,3).

The genetic material of phages is composed of either DNA or RNA and may be double- or single-stranded; however, a vast majority of characterized phages utilize dsDNA (4). Phage genomes (nucleic acids) are densely packaged and encompassed by an icosahedral protein capsid (4). From the small number of sequenced phage genomes collected, phages have been determined to be billions of years old and genetically diverse (5). Phage genomic architectures and sequences have distinct evolutionary histories and a mosaicism that suggests extensive horizontal genetic transfer (6).

There are three virion morphologies of dsDNA phages: *Myoviridae,* contractile tails built on a base plate*; Podoviridae*, very short tails; and *Siphoviridae,* long non-contractile tails (4). Phages are prevalent in many environmental conditions and are an excellent model for genuine scientific discovery; undergraduate students can generate hypotheses about uncharacterized phages for research opportunities (7).

Some phages are strictly lytic while others are termed "temperate." In the lytic cycle the bacteriophage infects the host bacteria cell, uses the cell's replication machinery to produce progeny phage, and leaves the cell after cell lysis. There are five stages of the lytic cycle: attachment, entry, phage replication DNA transcription/translation, assembly, and lysis. Attachment of the phage occurs when the phage tail proteins bind to specific receptors on the host cell's surface. The bacteriophage injects its dsDNA into the cytoplasm of the host bacteria

cell. The host cell's replication, transcription and translation machinery is forced to make copies

of the phage's viral genome as well as viral proteins. Packaging of the viral genome into

assembled protein capsids produces progeny phage particles. To lyse the bacterium, phage-

encoded proteins that perforate the plasma membrane and the cell wall are expressed (8). Once

the cell is lysed, progeny phage are released and can infect nearby cells (figure 1).
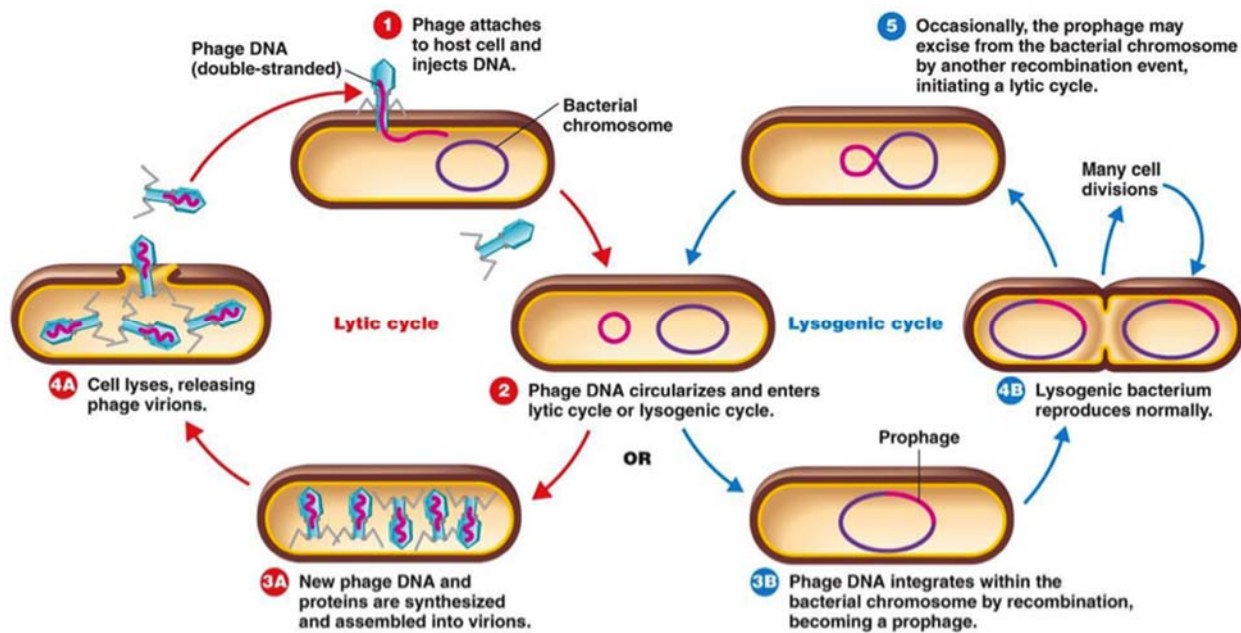
Figure 1. Bacteriophage Lifecycles.
A diagram of the lytic and lysogenic lifecycles that bacteriophages can undergo (8).

A subset of phages, termed "temperate" can undergo both the lytic or the lysogenic

lifecycles. In the lysogenic cycle, once the bacteriophage DNA enters the host the cell the phage

DNA is recombined into the bacterial host's chromosome (8). Integration of the phage genome

into the host bacterial chromosome occurs by phage-encoded integrase proteins. Integrase

proteins are site-specific recombinases that recognize short sequences of DNA (~30-40 bp) (9).

Bacteriophage integrases mediate recombination between phage DNA at the phage attachment

site, a sequence of bases known as *attP,* and bacteria DNA, the bacterial attachment site, a

sequence of bases known as *attB* (figure 2) (9). After the bacteriophage's genome is integrated

within the bacterial host chromosome it is flanked by the sites *attL* and *attR* (9). The *attL* and

attR sites are considered hybrid because they contain both the partial *attP* sequence and *attB*

sequence (figure 2) (9).
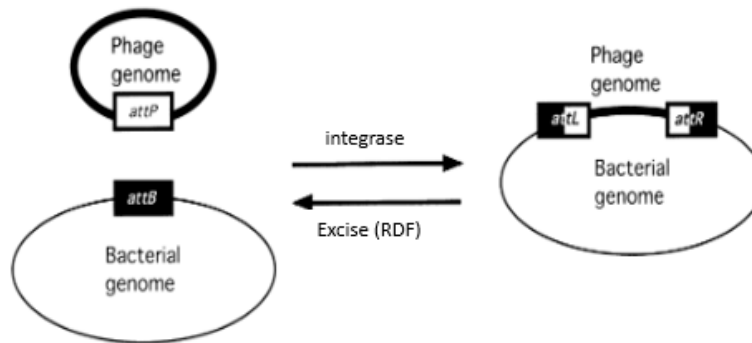
Figure 2. Diagram of Integration/Excision Event.
A schematic of bacteriophage genome integration and excision events into and out of host bacterial genome
mediated by integrase and excise proteins (10).

The integrated phage DNA is termed a prophage and its lytic genes are not expressed to drive

production of new phage particles; however, prophages are still copied with the host

chromosome DNA allowing the phage genome to still be reproduced. Some phages can switch

from the lysogenic cycle to the lytic cycle under stressful environmental conditions or

stochastically; in both cases the prophage is excised from the host chromosome (9). The *attL* and

attR sequences are recognizable by excise, a Recombinational Directionality Factor (RDF)

(Figure 4) (10,11). The RDF promotes prophage excision by redirecting the integrase to the *attL*

and *attR* sequences (11). After excision from the host chromosome, the phage DNA triggers the

remaining steps in the lytic cycle (figure 2).

1.2. Antibiotic Resistance

Since the early 1900s, antibiotics have been widely used to treat bacterial infections. Antibiotics are defined as molecules that inhibit the growth of or kill microorganisms (11). Penicillin, which is produced from a fungus, was first discovered by Alexander Fleming in 1928. Since the discovery of antibiotics, there has been the anticipation of antibiotic resistance. During Fleming's Nobel Peace Prize lecture in 1945 (awarded for the discovery of penicillin), he warned of the possibility of antibiotic resistance, "Then there is the danger that the ignorant man may easily under-dose himself by exposing his microbes to non-lethal quantities of the drug make them resistant (12)." The Centers for Disease Control and Prevention (CDC) states that penicillin-R *Staphylococcus* was identified as antibiotic resistant in 1940, three years prior to penicillin's introduction to hospitals in 1943 (13). Antibiotic resistance is a consequence of natural selection following random mutation and/or horizontal gene transfer. Bacteria that are resistant to an antibiotic due to mutations(s) in a gene survive and pass on the resistant gene to other bacteria by horizontal gene transfer or to daughter cells by reproduction. A bacterium is classified as a multi-drug resistant bacterium, or a "superbug" if the bacterium carries several resistance genes. The overuse of antibiotics as well as lengthy administration periods contribute to the increase in antibiotic resistance (14). According to the CDC, each year in the United States, at least 2 million people are infected with antibiotic resistant bacteria, and for more than 23,000 people, the infection is lethal (13).

1.3. Bacteriophage Therapy

Shortly after phages were discovered, d'Herelle explored the possibility of treating bacterial infections with phages. d'Herelle used phages to treat avian typhosis in chickens, Shigella-associated dysentery (shigellosis) in rabbits, and bacillary dysentery in humans (shigellosis) (3).

Shortly after those experiments, British medical officer Colonel Morison used phage to treat cholera outbreaks in India from 1930 to 1935 (15). While phages were commonly used as antibacterial agents in the early 1900's, the discovery of penicillin in 1928 led to widespread abandonment of phages as therapeutic agents in Western medicine. The recent development of many drug-resistant pathogens has increased the interest to revive and develop phages to treat bacterial infections again. Strictly lytic phages are preferable to temperate phages as therapeutic agents because of their ability to effectively lyse the bacterial host compared to their temperate phage counterparts that allow their bacterial host to persist after the temperate phage DNA is integrated into the host genome (16).

Phages have advantages over traditional antibiotics for bacterial infections because they are ubiquitous and host specific. In order to use phages as therapeutic agents, well-characterized large phage collections and/or automated pipelines that quickly isolate and identify phages are necessary. Phage therapy represents a potential alternative to antibiotics; however, there is a lack of clinical studies that were established with quality study design, meaning that the results of most studies cannot be assessed as statistically significant. Prior to establishment of bacteriophage therapy in clinical settings, research must be conducted to determine their effectiveness and ensure that the phage therapy will not negatively affect the patient or elicit harmful immune responses. Phage therapy case studies have been performed in recent years under extreme circumstances as final attempts to save patients with severe bacterial infections when all other treatment options have failed. Other phage therapy studies have been termed phase I trials, to ensure the safety of administering phages without serious side effects. Phase II trials are needed to determine the effectiveness of phage therapy to garner FDA approval (16).

Conventional phage therapy is the topical, oral, or systemic administration of many copies of one type of bacteriophage that specifically infects the bacterial infection of the patient. However, to reduce the emergence of phage resistant mutants, it is ideal for a bacteriophage cocktail (two or more types of phages) to be used at once or to administer the bacteriophage along with an antibiotic. Phage cocktails can be specifically tailored to infect more than one bacterial species. Phage cocktails can also be used to prevent the development of phage resistant mutants during treatment of bacterial infections. The co-administration of a phage and an antibiotic requires the host bacterial cell population to perform evolutionary trade-offs that likely result in reduction of infection (16).

A recent phage therapy study published by Strathdee and colleagues (2017) was conducted on a 68-year-old diabetic male who exhibited necrotizing pancreatitis complicated by a multi-drug resistant *Acinetobacter baumannii* infection. After a chosen bacteriophage cocktail was tested and shown to infect the patient's specific bacterial strain, the phage cocktail was administered intravenously and percutaneously. Results of the phage therapy study were promising, showing complete clearance of the bacterial infection (17).

Another recent bacteriophage therapy study by Hatfull and colleagues (2019) was conducted on a 15-year-old female with cystic fibrosis with a disseminated multi-drug resistant *Mycobacterium abscessus* infection. Three phages, Muddy, ZoeJ, and BPs, originally isolated on *Mycobacterium smegmatis* were determined to also infect the patient's specific bacterial strain. After six-months of intravenous administration, twice daily (10^9 phage particles per dose) of the cocktail of wild-type Muddy and engineered lytic derivates of ZoeJ and BPs, the patient showed

clinical improvement including sternal wound closure, improved liver function, and substantial improvement of infected skin nodules (18).

1.4. Methicillin- Resistant *Staphylococcus aureus*

Methicillin-resistant *Staphylococcus aureus* (MRSA) infections are a global health concern (19). *S. aureus* can cause complicated infections and are associated with high rates of morbidity and mortality. In industrialized nations, *S. aureus* is the leading cause of bacteremia, which often causes metastatic infections such as infective endocarditis, arthritis, and osteomyelitis (20). *S. aureus* bacteremia can progress to complications such as sepsis and/or septic shock.

Annually in the United States, about 90,000 individuals suffer from MRSA infections and about 20,000 of those infections are lethal (20). The CDC states that approximately 5% of patients in hospitals in the U.S. carry MRSA in their nose or on their skin (22). A review of 15 studies established that between 13 and 74 % of worldwide *S. aureus* infections are resistant to methicillin. The prevalence of MRSA isolates in Europe exhibits a north-south variation, and 7 of the 29 European countries still report at least 25 % of invasive *S. aureus* isolates are methicillin-resistant. In the US, it was estimated in 2005 that 31.8 per 100,000 people were infected by MRSA and 75% of those infections resulted in *S. aureus* bacteremia (20).

The incidence of MRSA infections is greatest from healthcare-associated onset acquired infections. Patients with MRSA infections obtained from healthcare-associated onset often exhibit comorbidities such as diabetes, decubitus, ulcers, chronic renal disease, prior stroke, and dementia. The healthcare-associated MRSA strains are commonly associated with pulsed-field gel electrophoresis (PFGE) USA100 or USA 200 strains and the community-associated MRSA strains are commonly associated with the USA300 or USA400 strains (20).

The community-associated strains have a higher expression of toxin producing genes when compared to the healthcare acquired strains, suggesting that the community-associated strains are more virulent. Colonization of non-invasive MRSA occurs in 1.3 % of the general population, the most common site of colonization is the anterior nares, MRSA may also colonize the throat, axilla, rectum, groin, or perineum (20).

1.5. JB Bacteriophage

Bacteriophage JB, isolated from dairy cow hair samples by Dr. Nygaard at Montana State University in the Voyich lab, has the ability to infect methicillin-resistant *S. aureus* USA300 strain LAC. JB's siphoviridae morphology was observed with a transmission electron microscope (figure 3). The icosahedral capsid was measured at a width of 75 nm, and the non-contractile tail length as 160 nm (figure 3) (21).
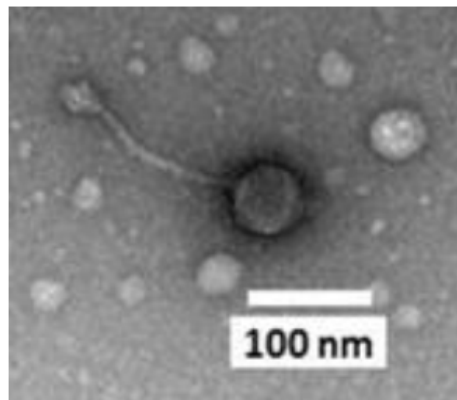
Figure 3. Transmission Electron Micrograph of JB.
JB's siphoviridae morphology captured by Transmission Electron Microscopy (21).

DNA sequencing and genome annotation characterized JB's genome as a circularly permuted 42,683 bp genome with 68 putative protein coding genes, and a G/C content of 35.2% (figure 4) (21).
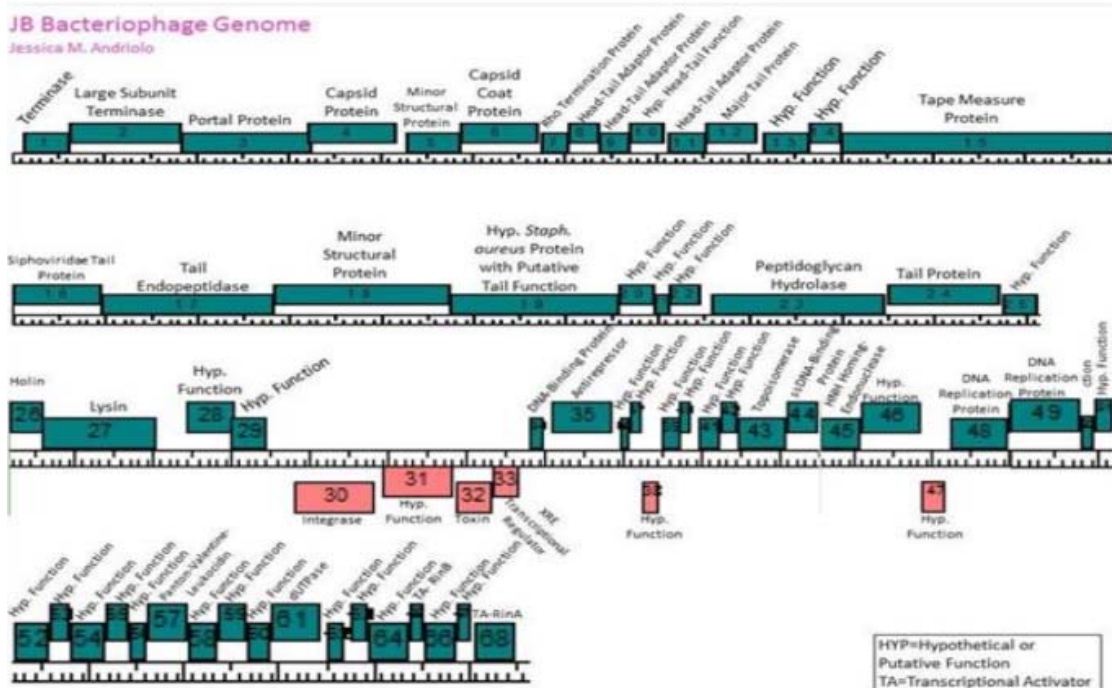
Figure 4. Genome Map.
JB bacteriophage's annotated genome map cropped into four tiers. Bioinformatically called genes are depicted by the green and red boxes spanning the length of the genome (21).

1.6. CRISPR-Cas9

Genetic modification and editing are important biotechnological research tools used to understand gene functions and biological mechanisms. In the past, gene editing used tools such as restriction enzymes, recombinases, programmable nucleases, and zinc finger nucleases; however, these gene editing tools were complex and/or limited in their specificity (22). Once the Clustered Regularly Interspaced Short Palindromic Repeats (CRISPR)/Cas (CRISPR associated)9 technology that utilized a single programmable guide RNA (sgRNA) (composed of crRNA and tracrRNA) was developed by Doudna and colleagues, genomic engineering became simplified and specific, eliminating the complexity that previously hampered genetic editing (23). In the past eight years since the newly developed CRISPR-Cas systems were first harnessed as powerful genomic editing tools, the CRISPR systems have allowed researchers to use the

CRISPR systems in a wide variety of applications from developing novel genome engineering

programs to clinical trials involving their potential therapeutic applications (22).

CRISPR-Cas9 systems are protein-nucleic acid complexes that provide bacteria and

archaea adaptive immunity from invasion by foreign nucleic acids such as phages (24). There are

three known types of CRISPR/Cas systems, Type I, II, and III (24). In nature, CRISPR systems

are a type of adaptive immune system that use small CRISPR RNAs (crRNAs) and Cas

nucleases to cleave foreign nucleic acids (24). The system is adaptive because it captures and

integrates foreign nucleic acid sequences (30-40 nucleotides) called "spacers" into its CRISPR

loci, between the partially palindromic DNA repeats of crRNA (24). When the foreign nucleic

acid sequence invades the cell, the host cell liberates the crRNAs and combines with a Cas

protein to form an effector complex that recognizes the nucleic acid sequence (protospacer) that

is complimentary to the crRNA (24).

The type II Cas9 system is the most used CRISPR-Cas system for genome editing. The crRNA

of this system relies on tracrRNA (trans-activating RNA), which has complimentary sequence to

the repeat-derived sequences in crRNA (24). The tracrRNA and the precursor crRNA base pair

to form a mature crRNA and associate with the Cas9 enzyme to form a complex (24). The

mature crRNA recognizes a short motif known as a protospacer adjacent motif (PAM) in the

target DNA sequence and guides the Cas9 enzyme to the target DNA sequence to create the

dsDNA break (24).

In many of the CRISPR/Cas systems a PAM sequence is absent from the host genome

but preserved in the foreign genome, thereby distinguishing between self and non-self (24). In

the Type II systems, the PAM is a consensus sequence that occurs downstream of the crRNA

binding sequence within the target DNA (24). The PAM sequence is essential for the Cas9

enzyme to introduce dsDNA breaks, and is required to license duplex unwinding, strand

invasion, and the formation of an R-loop structure (24). The Cas9 protein contains domains that

are homologous to HNH and RuvC-like endonucleases, and each domain cleaves one strand of

DNA. The HNH domain cleaves the DNA strand that is complimentary to the sgRNA and

the RuvC-like domain cleaves the non-complimentary DNA strand (24).

tracrRNA substantially enhances the specificity and binding of the Cas9 protein to target

DNA. Cas9 systems alone or Cas9-cRNA have decreased DNA binding at target sequences,

indicating that tracrRNA enhances target DNA recognition by orienting the crRNA correctly so

interaction with the complementary strand of DNA can occur. In nature, species that

have maintained specificity of dual RNA-guided cleavage of DNA indicate that Cas9, tracrRNA

and crRNA repeat have co-evolved. Additionally, efficient target DNA cleavage occurs

when there is a contiguous stretch of at least 13 base pairs between the crRNA and the target

DNA site proximal to the PAM (24).

Doudna and colleagues (2012), harnessed the CRISPR-Cas9 system to direct the

Cas endonuclease to a target sequence of plasmid DNA that bears a protospacer sequence

complimentary to a mature crRNA and a PAM sequence (23). Genomic editing nucleases, such

as the Cas9 nuclease, take advantage of innate cellular DNA repair systems (23). The nucleases

generate the DNA breaks that induce cellular damage responses such as non-homologous end-

joining (NHEJ) or homology-directed repair (HDR) (22). NHEJ response is error-prone and

often leads to insertion or deletion mutations (indels) within the DNA (22). NHEJ is often

induced to create gene knockouts by introducing a Cas9 cleavage to an exon to generate frame-

shift mutations to prematurely introduce stop codons and disrupt gene expression

(22). Megabase-size deletions can also be created by two targeted, double-stranded breaks and

relying on NHEJ to introduce a large deletion (22). HDR is less error prone; HDR is induced

after introduction of the Cas9 nuclease and a repair template to the target sequence of DNA. The

homology-directed repair can result in precise genome alterations such as the deletion of large

sequences (figure 5) (22).
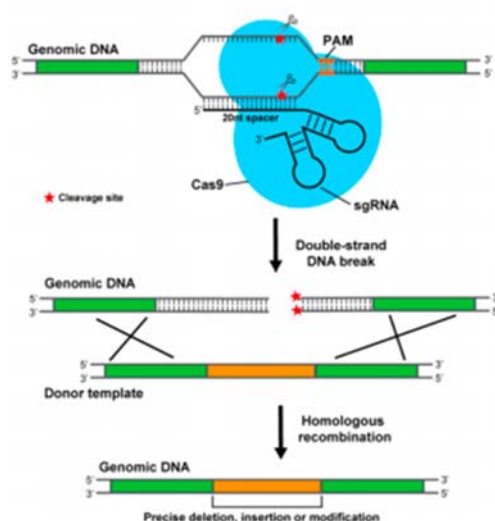
Figure 5. Schematic of CRISPR/Cas9 Deletion, Insertion, or Modification Event.
CRISPR/Cas9 creates a double stranded break upstream of the PAM sequence within the target DNA sequence. Homologous recombination of the genomic DNA with the provided donor template results in a precise deletion, insertion, or modification (22).

Doudna and colleagues devised an effective and simple method to program the Cas9

endonuclease family with a single guide RNA molecule that directs the Cas enzyme cleavage of

specific sequences of DNA to generate dsDNA breaks for genome targeting and editing (23).

1.7. Genomic Editing of Bacteriophages with CRISPR/Cas9

The recent ability to harness CRISPR-Cas9 as a tool for genomic engineering, allows

researchers to efficiently edit bacteriophage genomes to characterize and understand gene

functions. In nature, CRISPR systems are abundant in a broad range of species (23). The

CRISPR system is adaptive because it captures and integrates foreign nucleic acid sequences

(30-40 nucleotides) called "spacers" into its CRISPR loci, between the partially palindromic DNA repeats of crRNA (23). When foreign nucleic acid sequence invades the cell, the host cell generates crRNAs that combine with a Cas protein to form an effector complex which recognizes the nucleic acid sequence (protospacer) complimentary to the crRNA (23). Bacteriophage genomes can be modified to a desired construct by providing a donor DNA segment that bears the desired mutations within the protospacer region flanked by sequences that are homologous to the phage genome on both sides (22). To construct the desired mutant, the host cell uses the donor DNA segment after the Cas9 cleavage as a template for homologous recombination (22).

Chen and colleagues designed and constructed a CRISPR/Cas9 expression plasmid, pCasSA, to harness the CRISPR/Cas9 system for genomic editing in *S. aureus* (28). The pCasSA plasmid contains a strong *S. aureus rpsL* promoter to drive the expression of the Cas9 protein, a strong *cap/1A* promoter to drive the expression of the gRNA, a *BsaI* cloning site for the assembly of spacers, a *XbaI/Xhol* cloning site for repair arms, a chloramphenicol (Cm) resistance marker for screening in *S. aureus*, a kanamycin (KanR) resistance marker for screening in *E.coli*, *repF,* a temperature sensitive origin of replication for *S. aureus*, and ColE1, a replication origin for *E. coli* (figure 6) (28).
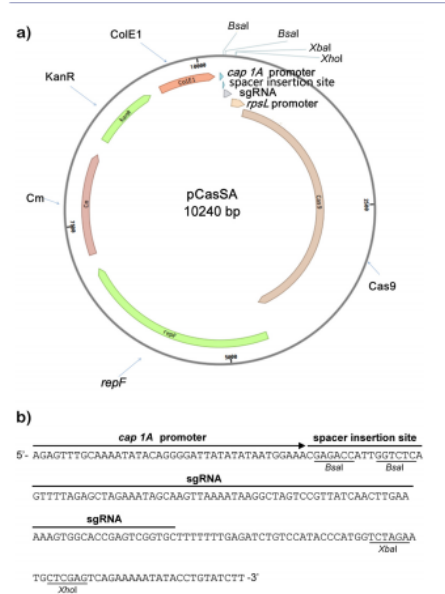
Figure 6. pCasSA plasmid.
pCasSA vector map of the cloning sites and antibiotics resistance markers. The XbaI and XhoI sites are available for the insertion of repair arms DNA sequence and the BsaI sites are available for the insertion of gRNA sequence (28).

JB phage contains a putative gene encoding for an integrase protein; the presence of this gene indicates that JB is likely a temperate bacteriophage. In order for JB to be used for therapeutic purposes, it is critical that a high proportion of phage infections results in bacterial cell lysis is critical for eradication of MRSA bacterial infections. It is therefore essential to delete the integrase gene in JB phage in order to create a strictly lytic JB phage derivative.

Within phage genomes it is not uncommon to find genes that encode putative toxin proteins. Abedone and LeJeune (2005) suggest that through genetic symbiosis between phage and bacteria after genome integration, toxin genes have remained prevalent in phages. These virulence factors contribute to the development of infectious diseases in eukaryotes (24). JB phage encodes a putative toxin protein; through CRISPR-Cas9 gene editing technology it is possible to remove the toxin gene, which is a necessary step before the JB phage could be used therapeutically in humans to treat MRSA bacterial infections.

1.8. Project Aims

Experiments were designed using repair arms to delete the cluster of four reverse genes (genes 30-33) within the JB genome after CRISPR-Cas9 mediated breaks (figure 7).
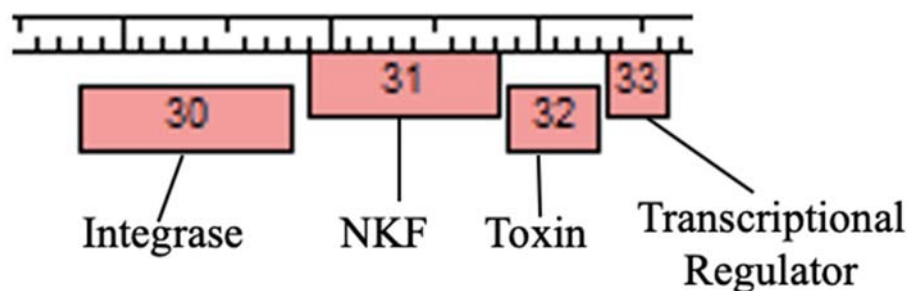
Figure 7. Schematic of the four genes to be deleted from the JB genome.

Gene number 30- putative integrase, Gene number 31- hypothetical protein with no known function, Gene number 32- putative toxin, Gene number 30- putative transcriptional regulator.

1.9. Experimental Design

A series of steps were planned to (1) construct a plasmid with gRNA and repair arms (figure 8); (2) introduce the plasmid into *S. aureus* RN4220*;* (3) infect the strain harboring the plasmid with the JB bacteriophage (figure 9); (4) isolate released phages by plaque assay on *S. aureus* PS88; and (5) screen resultant plaques for JB bacteriophage deletion mutant with PCR and DNA sequencing.
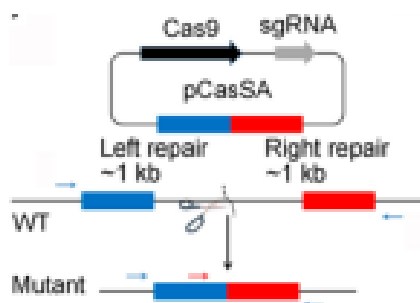
Figure 8. pCasSA-mediated genome editing.

Schematic of target DNA genomic editing after the introduction of the repair arms and sgRNA into the pCasSA plasmid (25).
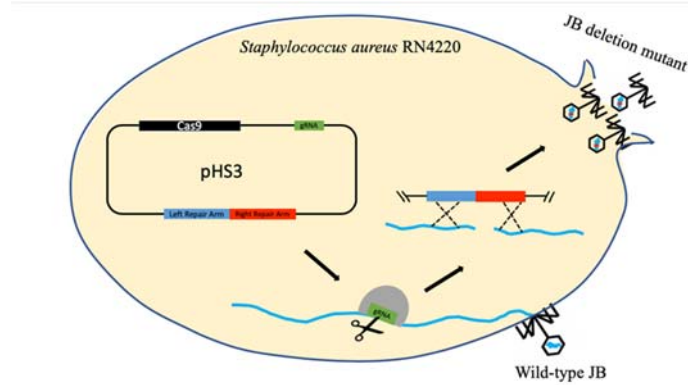
Figure 9. Phage Engineering.

Schematic of phage engineering after incorporation of the CRISPR/Cas9 expression vector into *S. aureus* RN4220. Expression of the Cas9 complex within *S. aureus* RN4220 after infection with the JB phage results in a double-stranded break within the JB DNA sequence that is homologous to the gRNA. Homologous recombination with the provided repair arms results in a deletion mutant JB phage (24).

2. Methods

2.1. Preliminary bioinformatic analysis of genes 30-33 within the JB bacteriophage genome

Initial JB phage genome annotation by Dr. Gregory determined the location and starts of genes 30-33 and their protein coding potential (21).

Additional bioinformatic analysis of genes 30-33 was done with the NCBI database, Basic Local Alignment Sequence Tool (BLAST) (25). Protein BLAST (BlastP) was performed by inputting genes 30-33's amino acid sequences into the BlastP tool (25). The BlastP compared the protein sequences of genes 30-33 to sequence databases and calculated the statistical significance of sequence alignment (25).

2.2. Construction of the pHS1 plasmid

2.2.1. Purification of the pCasSA plasmid

pCasSA, CRISPR-based *E. coli/S. aureus* temperature-sensitive plasmid for genome editing in *S. aureus* was purchased from Addgene (Addgene plasmid #982111; http://n2t.net/addgene:98211; RRID: Addgene_98211) (26) (figure 10).
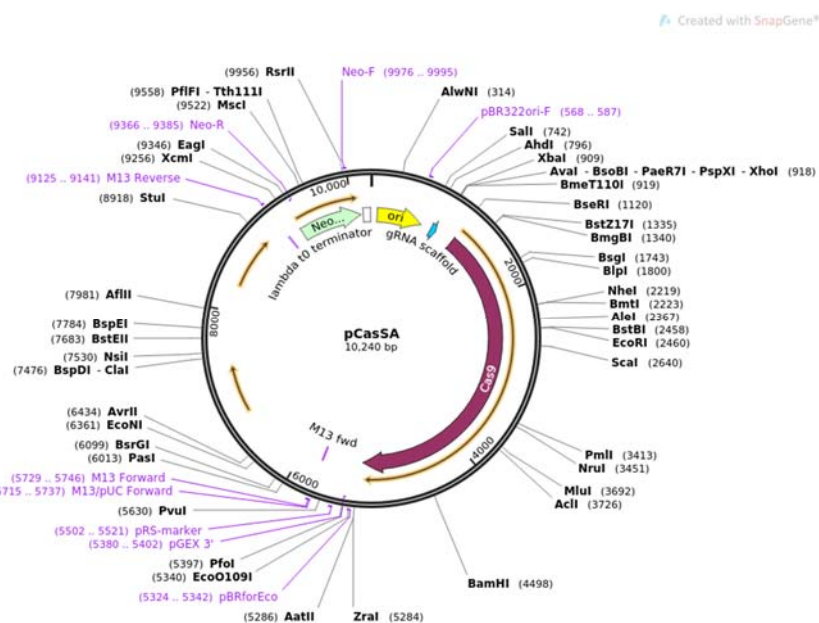
Figure 10. pCasSA (28).
A vector map of the pCasSA plasmid from Addgene.

The pCasSA plasmid was received within *Escherichia coli* in a bacterial agar stab. A sterile pipette tip was inserted into the bacterial agar stab, and the *E. coli* containing the plasmid were streaked using sterile technique onto a Luria Broth (LB) plate containing 50 µg/mL kanamycin. The plate was incubated at 37°C overnight. Isolated colonies were observed and picked into 4 mL of LB broth containing 50 µg/mL kanamycin and incubated overnight at 37°C with shaking at 250 rpm. The bacterial cultures were pelleted by centrifugation at 12,000 rpm for 5 minutes. The supernatant was decanted, and the plasmid was purified from the pelleted cells using a Thermo Scientific GeneJET Plasmid Miniprep Kit (K0503).

2.2.2. DNA Sequencing of pCasSA as a negative control for repair arms and gRNA

Purified pCasSA plasmid (100 ng/µL in a total volume of 10 µL) and aliquots of primers A, D, and F (50 ng/µL in a total volume of 10 µL) were sent to Functional Biosciences™ for DNA sequencing.

2.2.3. Amplification and Purification of the Left and Right Repair Arms

The JB bacteriophage genome six-frame translation and the genome annotation were used to determine the location of the four genes to be knocked out (19). Flanking left and right repair arm sequences were chosen (~1 kb each) (Appendix A). Primers to isolate the repair arms from the JB genome using polymerase chain reaction (PCR) were designed with flanking sequences for seamless cloning into the pCasSA plasmid's XbaI and XhoI cloning sites using NEBuilder Hifi DNA Assembly (Appendix B).

JB bacteriophage was amplified on *S. aureus* PS88 Rosenbach (ATCC 33742). The lysate was diluted 1:1000 in sterile nuclease-free water for use as a DNA template in the PCR reaction. PCR amplification of the left arm was performed by adding 1 µL JB lysate (5.0×10^5 pfu/mL) diluted in sterile nuclease-free water (1:1000), 12.5 pmol of primer A (Appendix B), 12.5 pmol of primer B (Appendix B), and 12.5 µL of Promega 2X GoTaq Green Mastermix and the final volume was brought to 25 µL. PCR amplification of the right arm was performed by the addition of 1 µL JB lysate (1:1000) diluted in sterile nuclease-free water, 12.5 pmol of primer C, 12.5 pmol of primer D, and Promega 2X GoTaq Green Mastermix for a final volume of 25 µL. The reactions were placed in a Bulldog Bio LifeECO Thermal Cycler [1 cycle (96°C -2 min.); 30 cycles (96°C- 15 sec., 60°C- 45 sec, 72°- 1 min 30 sec); 1 cycle (72°C- 5 minutes); indefinite hold at 4°C].

The reaction products were analyzed by agarose gel electrophoresis on a 0.8% agarose gel stained with 4×10^{-4} mg/mL EtBr at 130 V in 1X TBE Buffer. Ten microliters of the PCR products were flanked by 0.5 µg/lane of 1 KB GeneRuler Ladder. DNA bands were visualized on a Bio-Rad Gel Doc XR.

To purify the left and right repair arm PCR products, the bands were excised from the gel with sterile scalpels. The bands were purified using the ThermoFisher GeneJET Gel Extraction

Kit (K0692). To verify efficient recovery of the left and right repair arm DNA fragments, 5 uL

the purified products plus 1 µL of 6X loading dye were analyzed by agarose gel electrophoresis

flanked by 0.5 µg/lane of 1 KB GeneRuler Ladder on a 0.8% agarose gel stained with $4\text{x}10^{-4}$

mg/mL EtBr at 130 V in 1X TBE Buffer. DNA bands were visualized on a Bio-Rad Gel D XR.

2.2.4. Annealing of the Left and Right Repair Arms

For efficient cloning of the repair arms into the pCasSA plasmid, the purified

PCR products of the left and right repair arms were annealed using the NEBuilder Hifi DNA

Assembly Cloning Kit (NEB #E5520). The annealed product was diluted (1:10) in sterile

nuclease-free water and used as a DNA template for PCR. PCR amplification of the annealed

arms was performed by adding 1 µL annealed product (1:10), 12.5 pmol of primer A (Appendix

B), 12.5 pmol of primer D (Appendix B), and 12.5 µL of Promega 2X GoTaq Green Mastermix

in a final volume of 25 µL. The reactions were placed in a Bulldog Bio LifeECO Thermal

Cycler [1 cycle (96°C -2 min.); 30 cycles (96°C- 15 sec., 60- 45 sec, 72^0- 1 min 30 sec); 1 cycle

(72°C- 5 minutes); indefinite hold at 4°C]. To verify successful annealing of the left and right

repair arms, 5 µL the annealed product, plus 1 µL of 6X loading dye were analyzed by agarose

gel electrophoresis flanked by 0.5 µg/lane of 1 KB GeneRuler Ladder on a 0.8% agarose gel

stained with $4\text{x}10^{-4}$ mg/mL EtBr at 130 V in 1X TBE Buffer. DNA bands were visualized on a

Bio-Rad Gel Doc XR.

2.2.5. Insertion of the Repair Arms into the pCasSA plasmid

Two micrograms of the pCasSA plasmid were digested with 1 unit of XbaI (New England

BioLabs) and 5 µL of 10X Cutsmart Buffer (New England BioLabs) in a 50 µL reaction. The

reaction was incubated at 37°C for one hour, and 1 unit of XhoI (New England BioLabs) was

added for a sequential digest. The reaction was incubated at 37°C overnight. The digestion

reaction was purified using the QIAquick PCR Purification kit. To maintain the correct pH of the purification product, 10 µL of 3M NaOAc was added to the sample to ensure binding of the plasmid to the column. To confirm efficient digested plasmid recovery, 5 µL of the purified product was analyzed by agarose gel electrophoresis, next to one lane (0.5 µg/lane) of 1 KB NEB ladder and electrophoresed on a 0.8% agarose gel stained with 4×10^{-4} mg/mL EtBr in 1X TBE Buffer. DNA bands were visualized on a Bio-Rad Gel Doc XR.

The annealed repair arms were inserted into the vector at a 1:2 ratio using the NEB Hifi DNA Assembly Kit (NEB #E5520). The assembly reaction (2 uL) was subsequently transformed into NEB 10-beta Competent *E. coli* (High Efficiency, NEB #C3019). The transformed cells were plated with sterile glass beads on LB plates with 50 µg/mL kanamycin and incubated at 37°C overnight. To isolate the pHS1 plasmid, half of each isolated colony was picked with a sterile pipette into 4 mL LB broth with 50 µg/mL kanamycin and incubated at 37°C with shaking at 250 rpm overnight. Bacterial cultures were pelleted by centrifugation at 12,000 rpm for five minutes. The supernatant was decanted and the plasmid was purified from the pelleted cells using a Thermo Scientific GeneJET Plasmid Miniprep Kit (K0503). The miniprep samples of pHS1 were stored at -20°C.

To screen the bacterial colonies for the pHS1 plasmid, the other half of each isolated colony was picked with a sterile pipette into 999 µL of sterile nuclease-free water. PCR amplification of the annealed arms was performed to screen the colonies for the pHS1 plasmid by adding 1 µL of the suspended colonies, 12.5 pmol of primer A (Appendix B), 0.5 uL of 25 µM of primer D (Appendix B), and 12.5 µL of Promega 2X GoTaq Green Mastermix in a final volume of 25 µL. The reactions were placed in a Bulldog Bio LifeECO Thermal Cycler [1 cycle (96°C -2 min.); 30 cycles (96°C- 15 sec., 60°C- 45 sec, 72^0- 1 min 30 sec); 1 cycle (72°C- 5

minutes); indefinite hold at 4°C]. The reactions were analyzed by agarose gel electrophoresis on a 0.8% agarose gel stained with $4x10^{-4}$ mg/mL EtBr at 130 V in 1X TBE Buffer. Ten microliters of the PCR reactions were flanked by 0.5 µg/lane of 1 KB GeneRuler Ladder. DNA bands were visualized on a Bio-Rad Gel Doc XR.

Cultures from colonies that were confirmed to contain the pHS1 plasmid were made into glycerol stocks; 500 µL of the bacterial culture was mixed with 500 µL of sterile 40% glycerol in a 2 mL cryovial. The glycerol stocks of *E. coli* containing pHS1 were stored at -80°C.

2.3. Construction of the pHS3 plasmid

2.3.1. Creation of the gRNA

To generate the pHS3 plasmid, a gRNA (Appendix A) was designed from the JB phage genome and ligated into the pHS1 plasmid. The gRNA was designed by identifying a sequence within the cluster of four genes to be knocked-out that was upstream of a PAM sequence 5' to 3 (located within gene 32 at 29,030-29,050). The oligonucleotides were designed and ordered from Integrated DNA Technologies (IDT) (Appendix A). The oligos were resuspended in sterile-nuclease free water to a concentration of 50 µM. The oligonucleotides were phosphorylated by adding 50 µM of primer F (Appendix B) and 50 µM of primer G (Appendix B) 1 µL of 10X T4 DNA ligase buffer, and 1 µL of 10 U/µL T4 polynucleotide kinase. The phosphorylation reaction was incubated at 37°C for one hour. After phosphorylation, the oligonucleotides were annealed by adding 2.5 µL of 1M NaCl to the phosphorylation reaction. The sample was transferred to a sterile PCR tube and the reaction was placed in a Bulldog Bio LifeECO Thermal Cycler at 95°C for 3 minutes and slowly cooled to room temperature. The annealed oligos were diluted 1:20 with sterile nuclease-free water.

2.3.2. Golden Gate Assembly

To introduce the gRNA into the pHS1 plasmid, Golden Gate Assembly was used. To a

sterile PCR tube, 2 µL of 20 fmol pHS1 plasmid, 1 µL of 100 fmol annealed oligos, 1 µL of 10X

T4 DNA ligase buffer, 0.5 uL of 1 U/uL T4 DNA ligase, and 0.5 µL of BsaI-HFv2 were added.

The Golden Gate assembly reaction was placed in a Bulldog Bio LifeECO Thermal Cycler at

(37ºC for 2 min, 16ºC for 5 min) for 25 cycles, followed by 50ºC for 5 min, 80ºC for 15 min, and

held at 10ºC.

2.3.3. Transforming *E. coli* with the pHS3 plasmid and screening

The pHS1/gRNA (pHS3) Golden Gate assembly reaction was subsequently transformed

into NEB 10-beta Competent *E. coli* (High Efficiency, NEB #C3019) using the NEBuilder Hifi

DNA Assembly Kit. The transformed cells were plated with sterile glass beads on LB plates with

50 µg/mL Kanamycin at 37ºC overnight. To purify the pHS3 plasmid, half of each isolated

colony was picked with a sterile pipette into 4 mL LB broth with 50 µg/mL kanamycin and

incubated with shaking at 37ºC at 250 rpm overnight. Bacterial cultures were pelleted by

centrifugation at 12,000 rpm for five minutes. The supernatant was decanted, and the plasmid

was purified from the pelleted cells using a Thermo Scientific GeneJET Plasmid Miniprep Kit

(K0503). The purified pHS3 plasmid was stored at -20ºC.

To screen the bacterial colonies for the pHS3 plasmid, the other half of each isolated

colony was picked with a sterile pipette into 999 µL of sterile nuclease-free water. PCR

amplification of a region in the plasmid between the left repair arm and gRNA was performed to

screen for the insertion of the gRNA and to confirm the creation of the pHS3 plasmid by adding

1 µL diluted colony (1:1000), 12.5 pmol of primer E (Appendix B), 12.5 pmol primer F

(Appendix B), and 12.5 µL of Promega 2X GoTaq Green Mastermix for a final volume of 25

µL. The reactions were placed in a Bulldog Bio LifeECO Thermal Cycler [1 cycle (96ºC -2 min.); 30 cycles (96ºC- 15 sec., 52ºC- 45 sec, 72^0- 1 min 30 sec); 1 cycle (72ºC- 5 minutes); indefinite hold at 4ºC].

The reactions were analyzed by agarose gel electrophoresis on a 0.8% agarose gel stained with 4x10^{-4} mg/mL EtBr at 130 V in 1X TBE Buffer. Ten microliters of the PCR reactions were flanked by 0.5 µg/lane of 1 KB GeneRuler Ladder. DNA bands were visualized on a Bio-Rad Gel Doc XR.

Cultures from colonies that were confirmed to contain the pHS3 plasmid were made into glycerol stocks, 500 µL of the bacterial culture were mixed with 500 µL of sterile 40% glycerol in a 2 mL cryovial. The glycerol stocks of pHS3 were stored at -80ºC.

2.4. Transformation of the pHS3 plasmid into *S. aureus*

2.4.1. Generating High Concentrations of Plasmids for electroporation into *S. aureus* RN4220

From the *E. coli* glycerol stock of the pCasSA plasmid, a small scraping was streaked onto an LBA plate containing 50 µg/mL kanamycin for isolated colonies and incubated overnight at 37ºC. Five isolated colonies were picked with a sterile pipette tip into 5 mL of LB containing 50 µg/mL kanamycin and incubated at 250 rpm at 37ºC overnight. The bacteria were pelleted by centrifugation for 5 minutes at 12,000 rpm. The supernatant was discarded and the pCasSA plasmid from the first culture was purified using the Thermo Scientific GeneJET Plasmid Miniprep Kit (K0503). The purified pCasSA sample from the first culture was used to elute the purified plasmid from the second culture of pCasSA. The pCasSA plasmid eluate was used to sequentially to elute the purified plasmid from the remaining columns to generate a high concentration (~500-1,000 ng/µL) of pCasSA plasmid for electroporation. The steps were repeated for the pHS1 and pHS3 plasmids.

2.4.2. Culturing *S. aureus* RN4220

The *S. aureus* RN4220 glycerol stock was stored at -80°C. From the freezer stock of *S. aureus* RN4220, a sterile pipette was used to add a small scraping of the *S. aureus* RN4220 glycerol stock to 20 mL of TSB. The culture flask was incubated at 37°C with shaking at 250 rpm overnight for 12 hours.

2.4.3. Generation of Electrocompetent *S. aureus* RN4220

Two sterile culture flasks containing 100 mL TSB were inoculated with 1 mL of overnight culture of *S. aureus* RN4220 and incubated at 37°C at 250 rpm until the OD_{600} reached 0.5 (~3 hours). The cells were transferred to four sterile 50 mL conical tubes and placed on ice for 15 minutes. The cells were pelleted by centrifugation at 12,000 rpm, 10 min, 4°C. The supernatant was removed and discarded without disturbing the pellet. Each aliquot was washed with 50 mL of ice-cold sterile deionized water. The cells were centrifuged for 10 minutes at 4,000xg at 4°C. The supernatant was removed and discarded without disturbing the pellet. The pellet was resuspended in 25 mL ice-cold sterile deionized water. Two resuspended bacterial pellets were combined into one 50 mL conical tube and centrifuged for 10 minutes at 4,000xg at 4°C. The supernatant was removed and discarded without disturbing the bacterial pellet. The two remaining pellets were resuspended in 16 mL ice-cold sterile 10% glycerol, and centrifuged for 10 minutes at 4,000xg at 4°C. The supernatant was removed and discarded without disturbing the bacterial pellet. The pellet was thoroughly resuspended with 1 mL ice-cold sterile 10% glycerol, and transferred to a sterile 1.5 mL microcentrifuge tube, and centrifuged for 5 minutes at 5,000xg at 4°C. The supernatant was removed without disturbing the bacterial pellet. The pellet was resuspended in 700 µL ice-cold sterile 10% glycerol. The bacteria were divided into pre-chilled 70 µL aliquots in 0.5 mL microcentrifuge tubes and frozen immediately at -80°C.

2.4.4. Transforming pHS3 into *S. aureus* RN4220 and screening

The electrocompetent cells were retrieved from the -80°C and thawed on ice for 10 minutes. TSA was aliquoted in 250 µL increments into 1.5 mL microcentrifuge tubes and pre-warmed at 37°C. To the thawed electrocompetent *S. aureus,* 1.2 ug of plasmid was added and gently mixed by pipetting. The transformation mixture was transferred to a pre-chilled ThermoFischer Scientific cuvette with a 0.2 cm electrode gap. The cuvette was placed in the sample chamber of a Bio-Rad Gene Pulser II/ Pulse Controller Plus/ Capacitance Extender Plus and pulsed once at 2.5 kV, capacitor at 25 µF, and parallel resistor at 200 Ohms, yielding a field strength of 12.5 kV and a time constant of -2.5 ms. The cells were immediately mixed into the 250 µL of pre-warmed TSB. The mixture was transferred to a sterile culture tube and incubated at 30°C at 500 rpm for 5 minutes and 250 rpm for 55 minutes. The aliquots were plated in 20 µL and 200 uL aliquots on TSA containing 10 µg/mL chloramphenicol for 36 hours at 30°C.

To screen the bacterial colonies for the pHS3 plasmid, 20 colonies were picked with a sterile pipette into 999 µL of sterile nuclease free water. PCR amplification of the left and right repair arms to confirm the structure of the pHS3 plasmid was performed by adding 1 µL resuspended colony, 12.5 pmol of primer A (Appendix B), 12.5 pmol of primer D (Appendix B), and 12.5 µL of Promega 2X GoTaq Green Mastermix to a final volume of 25 µL. The reactions were placed in a Bulldog Bio LifeECO Thermal Cycler [1 cycle (96°C -2 min.); 30 cycles (96°C- 15 sec., 60°C- 45 sec, 72^0- 1 min 30 sec); 1 cycle (72°C- 5 minutes); indefinite hold at 4°C]. The reaction products were analyzed by agarose gel electrophoresis on a 0.8% agarose gel stained with 4×10^{-4} mg/mL EtBr at 130 kV in 1X TBE Buffer; 10 µL of the PCR reactions, were flanked by 0.5 µg/lane of 1 KB GeneRuler Plus Ladder. DNA bands were visualized on a Bio-Rad Gel Doc XR.

Transformed colonies that were confirmed to contain the plasmid were picked with a sterile pipette into 3 mL TSB containing 10 µg/mL of chloramphenicol and incubated overnight at 250 rpm at 30ºC. The bacterial cultures were made into glycerol stocks: 500 µL of the bacterial culture was combined with 500 µL of sterile 40 % glycerol in a 2 mL cryovial. The glycerol stocks of plasmids were stored at -80ºC.

2.5. Infection of *S. aureus* RN4220-pHS3 with bacteriophage JB

2.5.1. Liquid infection of *S. aureus* RN4220-pHS3 with bacteriophage JB

An isolated colony of *S. aureus* RN4220-pHS3 was picked into 3 mL of 10 µg/mL kanamycin, TSB (supplemented with 25% dextrose and 0.1 M $CaCl_2$) and grown overnight at 30ºC with shaking at 250 rpm. An isolated colony of *S. aureus* RN4220 was picked into 3 mL of TSB++ and grown overnight at 30ºC with shaking at 250 rpm. Ten microliters of JB lysate (concentration of the JB lysate: 5.0 x 10^5 pfu/mL) and 3 mL of TSB (supplemented with 25% dextrose and 0.1 M $CaCl_2$) were added to 250 µL of *S. aureus* RN4220-pHS3 and incubated for 36 hours at 37ºC with shaking at 250 rpm. Ten microliters of JB lysate (5.0 x 10^5 pfu/mL) and 3 mL of TSB (supplemented with 25% dextrose and 0.1 M $CaCl_2$) were added to 250 µL of *S. aureus* RN4220 and incubated for two nights at 30ºC with shaking at 250 rpm.

2.5.2. Lysate creation of putative JB deletion mutant (JBΔ30-33)

After a 36-hour incubation, the liquid JB infection culture of *S. aureus* RN4220-pHS3 was centrifuged at 2,000 rpm for 5 minutes. Three milliliters of supernatant were filtered through a 0.22 µm filter into a sterile 15 mL conical tube.

2.5.3. Plaque Assay of *S. aureus* ATCC 33742 (PS88) with bacteriophage JB and putative deletion mutant JBΔ30-33

An isolated colony of *S. aureus* ATCC 33742 (PS88) was picked into 3 mL of TSB

(supplemented with 25 % dextrose and 0.1 M CaCl$_2$) and grown overnight at 30°C with shaking

at 250 rpm. Ten microliters of JB lysate (5.0 x 10^5 pfu/mL) and 3 mL of TSB (supplemented

with 25 % dextrose and 0.1 M CaCl$_2$) were added to 250 µL of *S. aureus* RN4220-pHS3 and

incubated at room temperature for 15 minutes. Five milliliters of molten top agar (65°C) of

TSTA (supplemented with 25 % dextrose and 0.1 M CaCl$_2$) , was added to the culture of *S.

aureus* RN4220 with JB phage and poured onto a TSA (supplemented with 25 % dextrose and

0.1 M CaCl$_2$) plate, after the top agar solidified, the plate was incubated overnight at 30°C. Ten

microliters of JB lysate (5.0 x 10^5 pfu/mL) and 3 mL of TSB (supplemented with 25 % dextrose

and 0.1 M CaCl$_2$) were added to 250 uL of *S. aureus* RN4220 and incubated at room temperature

for 15 minutes. Five milliliters of molten top agar (65°C) of TSTA (supplemented with 25 %

dextrose and 0.1 M CaCl$_2$) , was added to the culture of *S. aureus* RN4220 with JB phage and

poured onto a TSA (supplemented with 25 % dextrose and 0.1 M CaCl$_2$) plate, after the top agar

solidified, the plate was incubated at 30°C.

2.6. Confirmation of deletion mutant JBΔ30-33.

2.6.1. Screening plaques for deletion mutant JBΔ30-33 by PCR.

Plaques from JBΔ30-33 infection on *S. aureus* ATCC 33742 (PS88) were picked into 50

µL of sterile nuclease-free water. Plaques from wild-type JB infection of *S. aureus* ATCC 33742

(PS88) were picked into 50 µL of sterile nuclease-free water. An isolated colony of *S. aureus*

ATCC 33742 (PS88) was picked into 1000 µL of sterile nuclease-free water as a negative

control. Purified pHS3 was picked into 1000 µL of sterile nuclease-free water as a positive

control. PCR amplification of the left and right repair arms was used to confirm the presence or

absence of genes 30-33 within the JB phage genome. One microliter of template DNA

(resuspended plaque or plasmid control), 12.5 pmol of primer A (Appendix B), 12.5 pmol of

primer D (Appendix B), and 12.5 µL of Promega 2X GoTaq Green Mastermix and brought to a

final volume of 25 µL. The reactions were placed in a Bulldog Bio LifeECO Thermal Cycler [1

cycle (96°C -2 min.); 30 cycles (96°C- 15 sec., 60°C- 45 sec, 72^0- 1 min 30 sec); 1 cycle (72°C- 5

minutes); indefinite hold at 4°C]. The reactions were analyzed by agarose gel electrophoresis on

a 0.8 % agarose gel stained with 4×10^{-4} mg/mL EtBr at 130 kV in 1X TBE Buffer, 10 µL of the

PCR reactions, were flanked by 0.5 µg/lane of 1 KB GeneRuler Plus Ladder. DNA bands were

visualized on a Bio-Rad Gel Doc XR.

2.6.2. DNA sequencing of PCR amplicons from wild-type JB and JBΔ30-33.

PCR products of amplified sequence from putative deletion mutant JBΔ30-33, wild-type

JB, *S. aureus* ATCC 33742 (PS88), and sterile-nuclease free water (figure 28) were purified with

a QIAquick PCR purification kit. Purified PCR products and 10 µM aliquots of primers A, D,

and F were sent to Functional Biosciences™ for DNA sequencing.

3. Results and Discussion

3.1. Preliminary bioinformatic analysis of genes 30-33 within the JB bacteriophage genome

Annotated gene #30 is 1047 bp in length, 5' (26,799-27,845) 3' within the JB genome.

Bioinformatic analysis of gene #30 revealed that it putatively encodes for a site-specific

integrase. BlastP analysis of gene 30 confirmed significant alignment (>99 %) for several *S.*

aureus-encoded site-specific integrases (figure 11).

Sequences producing significant alignments:

Select: All None Selected:0

Description	Max Score	Total Score	Query Cover	E value	Per. Ident	Accession
site-specific integrase [Staphylococcus aureus]	718	718	99%	0.0	100.00%	WP_015978393.1
site-specific integrase [Staphylococcus aureus]	716	716	99%	0.0	99.71%	WP_050959874.1
MULTISPECIES: site-specific integrase [Staphylococcus]	715	715	99%	0.0	99.71%	WP_001145722.1
tyrosine-type recombinase/integrase [Staphylococcus aureus]	714	714	99%	0.0	99.14%	WP_154269489.1
site-specific integrase [Staphylococcus aureus]	714	714	99%	0.0	99.43%	WP_049302953.1
site-specific integrase [Staphylococcus aureus]	714	714	99%	0.0	99.43%	WP_044124126.1
site-specific integrase [Staphylococcus aureus]	714	714	99%	0.0	99.43%	WP_117232347.1
site-specific integrase [Staphylococcus aureus]	714	714	99%	0.0	99.43%	WP_064136105.1
site-specific integrase [Staphylococcus aureus]	714	714	99%	0.0	99.43%	WP_053865355.1

Figure 11. BlastP analysis of Gene 30.

Figure showing significant similarity of JB gene 30 protein sequence to site-specific integrases within the GenBank database.

Gene #31 is 930 bp in length, 5' (27,907-28,836) 3' within the JB genome. Bioinformatic

analysis of gene #31's gene product revealed that it putatively encodes domain-containing

protein without a known function. BlastP analysis of gene #31 protein sequence confirmed

significant alignment (>98 %) for several *S. aureus* domain-containing proteins (figure 12).

Figure 12. BlastP analysis of Gene 31.

Figure showing significant similarity of JB gene 31 product's amino acid sequence to domain-containing proteins within the GenBank database.

Gene #32 is 459 bp in length, 5' (28,855-29,313) 3' within the JB genome. Bioinformatic analysis of gene #32's product revealed that it putatively encodes a toxin protein. BlastP analysis of gene #32 protein sequence confirmed significant alignment (>98 %) for several *S. aureus-*encoded toxin proteins (figure 13).

Figure 13. BlastP analysis of Gene 32.

Figure showing significant similarity of JB gene 32 product's amino acid sequence to toxins within the GenBank database.

Gene #33 is 315 bp in length, 5' (29,335-29,649) 3' within the JB genome. Bioinformatic analysis of gene #33's product revealed that it putatively encodes a helix-turn-helix transcriptional regulator protein. BlastP analysis of gene #33's protein sequence significant alignment (>98 %) for several *S. aureus* encoded helix-turn-helix transcriptional regulator proteins (figure 14).

Sequences producing significant alignments:
Select: All None Selected:0

Alignments Download GenPept Graphics Distance tree of results Multiple alignment

Description	Max Score	Total Score	Query Cover	E value	Per. Ident	Accession
MULTISPECIES: helix-turn-helix transcriptional regulator [Staphylococcus]	216	216	99%	7e-71	100.00%	WP_001118607.1
helix-turn-helix transcriptional regulator [Staphylococcus aureus]	214	214	99%	3e-70	99.04%	WP_103147424.1
helix-turn-helix transcriptional regulator [Staphylococcus aureus]	213	213	99%	6e-70	99.04%	WP_001118608.1
MULTISPECIES: helix-turn-helix transcriptional regulator [Staphylococcus]	205	205	99%	1e-66	94.23%	WP_002504199.1
helix-turn-helix transcriptional regulator [Staphylococcus chromogenes]	169	169	98%	1e-52	77.67%	WP_107399204.1
helix-turn-helix transcriptional regulator [Staphylococcus petrasii]	169	169	99%	2e-52	76.92%	WP_103366890.1
MULTISPECIES: helix-turn-helix transcriptional regulator [Staphylococcus]	169	169	99%	3e-52	75.96%	WP_049387435.1

Figure 14. BlastP analysis of Gene 33.

Figure showing significant similarity of JB gene 32's amino acid sequence to helix-turn-helix transcriptional regulator proteins within the GenBank database.

3.2. Construction of the pHS1 plasmid

3.2.1. Purification of the pCasSA plasmid

Isolated colonies were grown from the *E. coli* bacterial stab on an LBA plate containing 50 µg/mL kanamycin suggesting the presence of the pCasSA plasmid (figure 15).

Figure 15. *E. coli* containing the pCasSA plasmid.
A streak plate showing isolated colonies of *E. coli* containing the pCasSA plasmid.

Following purification of the pCasSA plasmid from liquid cultures of the isolated

colonies of *E. coli*, Nanodrop™ analysis determined the concentration of the purified plasmid to

be 160.8 ng/µL with a 260/280 ratio of 1.95 (figure 16).
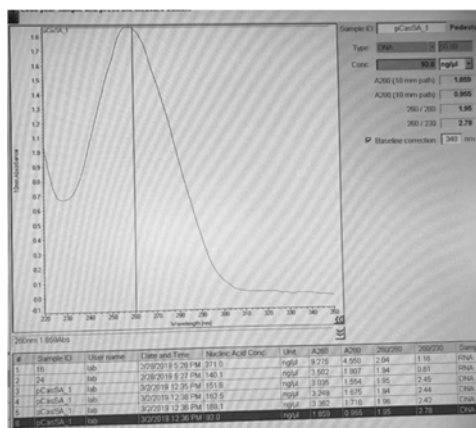
Figure 16. Purified pCasSA plasmid.
Graph and DNA concentrations of the pCasSA plasmid following Nanodrop™ analysis.

3.2.2. DNA sequencing of pCasSA as a negative control for repair arms and gRNA

To establish the purified plasmid lacked DNA sequences similar to JB Bacteriophage,

DNA Sequencing reactions were run. As expected, DNA sequencing of the purified pCasSA

plasmid did not produce a DNA sequence from primers A (figure 17). The sequencing results

show that the repair arms are not within the template pCasSA plasmid.
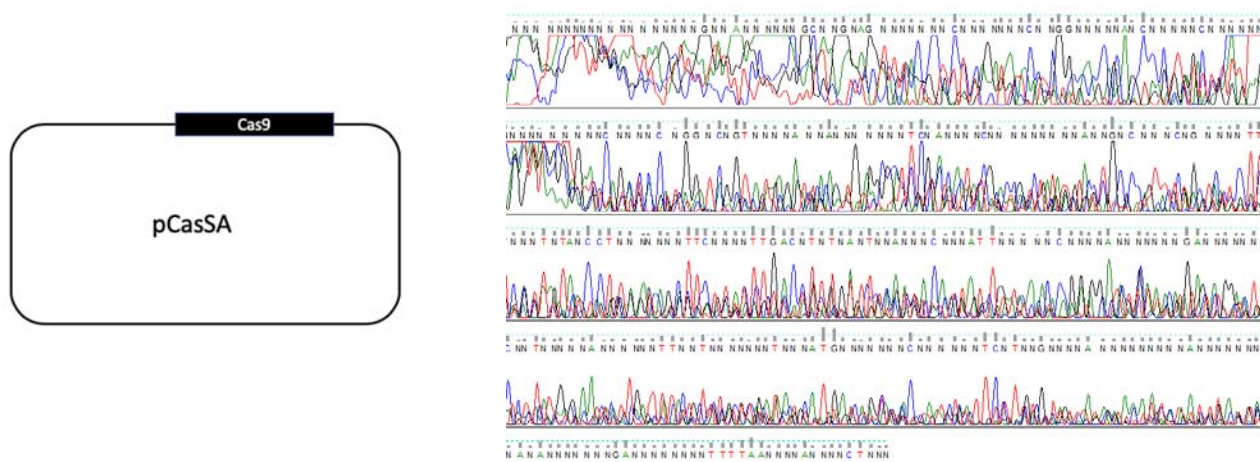
Figure 17. DNA Sequencing of pCasSA.
The figure shows sequencing results from pCasSA with primer A.

DNA sequencing of the purified pCasSA plasmid also did not produce a DNA sequence from primer F (figure 18). The sequencing results show that the gRNA is not within the template pCasSA plasmid.

Figure 18. DNA Sequencing of pCasSA.

The figure shows sequencing results from pCasSA with primer F.

3.2.3. Amplification and Purification of the Left and Right Repair Arms

Polymerase chain reaction amplification of the left and right repair arms yielded DNA bands at the expected sizes of 906 bp and 971 bp, respectively (figure 19). The gel electrophoresis image demonstrates the successful amplification of the left and right flanking sequences of the genes of interest (30-33).

Figure 19. Gel Electrophoresis Images of Left and Right Repair Arms.

Gel a.) Gel electrophoresis of left and right repair arms amplified from JB lysate with Polymerase Chain Reaction; L- GeneRuler 1 kb DNA ladder, 1- Left repair arm (expected size = 906 bp), 2- Right repair arm (expected size= 971 bp). Gel b.) Gel electrophoresis of left and right repair arms after excision and purification from gel a; L- GeneRuler 1 kb DNA ladder, 1- Left repair arm (expected size = 906 bp), 2- Right repair arm (expected size= 971 bp).
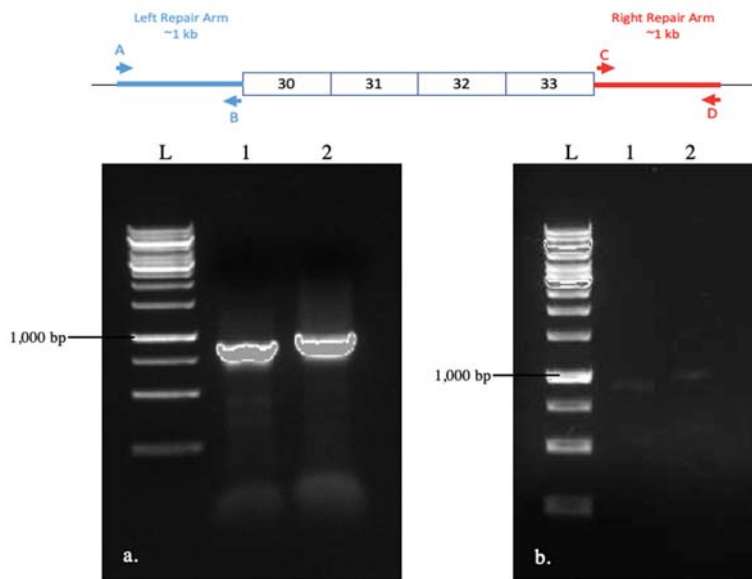
3.2.4. Annealing of the Left and Right Repair Arms

DNA assembly of the left and right repair arms yielded a DNA band at the expected size of 1,877 bp (figure 20). The presence of the band at 1,877 bp indicates that the left and right repair arms were covalently joined.
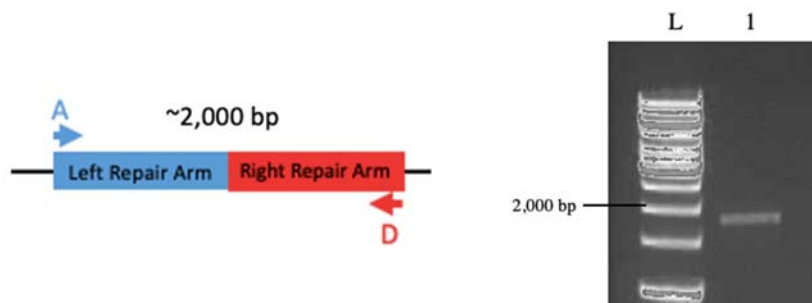

Figure 20. Gel Electrophoresis Images of Annealed Left and Right Repair Arms.

Gel electrophoresis of annealed repair arms after DNA assembly; L- GeneRuler 1 kb DNA ladder, 1-annealed left and right repair arms (expected size = 1,877 bp).

3.2.5. Insertion of the Repair Arms into the pCasSA plasmid

Supercoiled and circularized plasmids electrophoretic mobility vary from linear; purified

plasmids often show two bands (figure 21, lane 1). Linearization of the pCasSA plasmid

occurred after restriction enzyme digestion with XbaI and XhoI and was visualized with gel

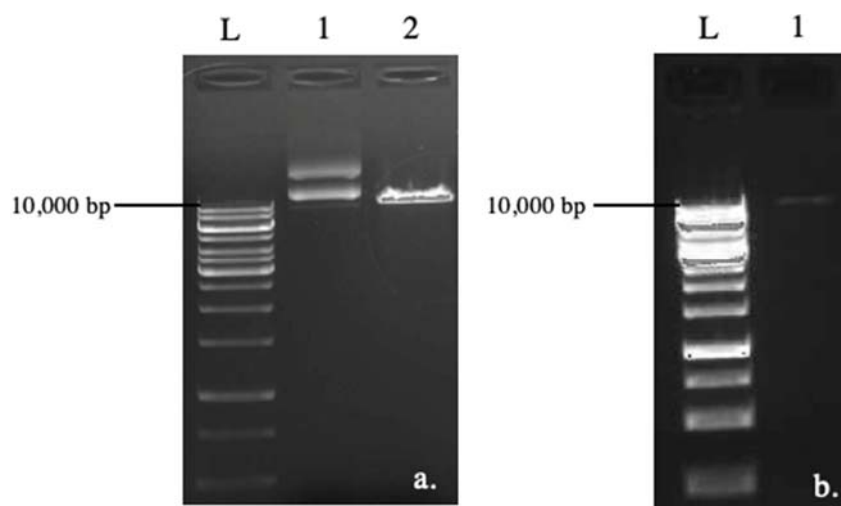electrophoresis. The linearized band was observed at the expected size of 10,231 bp (figure 21).

Figure 21. Gel Electrophoresis image of linearized pCasSA.
Gel a.) Gel electrophoresis of linearized pCasSA; L- GeneRuler 1 kb DNA ladder, 1- Circularized and supercoiled
pCasSA (expected size= 10,240 bp) 2- linearized pCasSA (expected size= 10,231 bp). **Gel b.)** Gel electrophoresis of
linearized pCasSA after excision and purification from gel a; L- GeneRuler 1 kb DNA ladder, 1- linearized pCasSA
(expected size = 10,231 bp bp).

To create pHS1, linearized plasmid and repair arms were joined by NEB Hi-Hi DNA

Assemby and transformed into *E. coli*. The resultant colonies of *E. coli* that putatively contained

the pHS1 plasmid grew on an LB plate containing 50 µg/mL of kanamycin (figure 22).

Figure 22. Colonies of *E. coli* putatively containing the pHS1 plasmid.
Left plate- Isolated colony growth of *E. coli* putatively containing pHS1. Right Plate- Negative control
plate with minimal colony growth.

Polymerase chain reaction to screen for the repair arms (expected size of 1,877 bp) of the

pHS1 plasmid within isolated *E. coli* colonies (figure 22) using primers A and D, revealed the

expected product size for the presence of the pHS1 plasmid within 16 of 20 picked colonies after

transformation (refer to figure 23). Colonies picked from the pCasSA (negative control plate)

(figure 22) did not yield bands for the repair arms. The positive controls of the purified

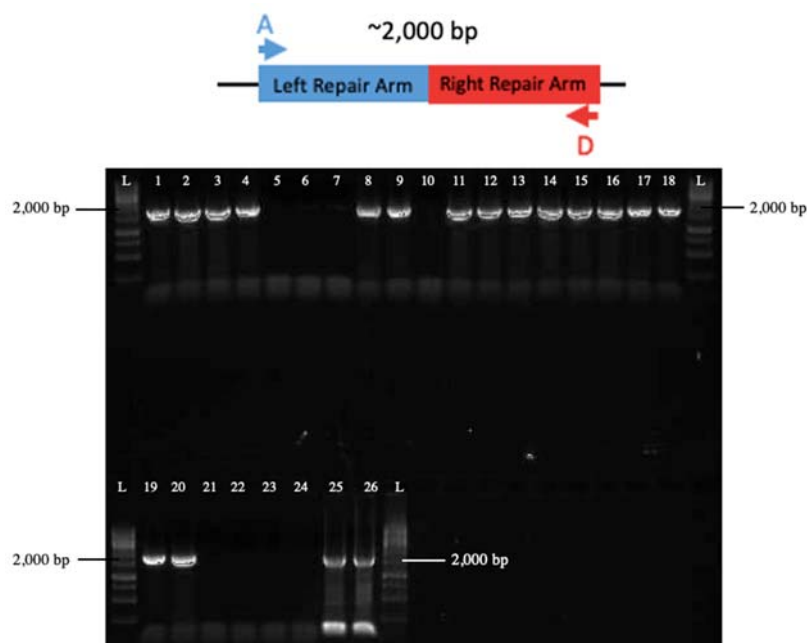assembled arms yielded bands of the expected size, 1,877 bp (figure 23).

Figure 23. Gel Electrophoresis of PCR products to screen for the presence of pHS1 within *E. coli*.

L- GeneRuler 1 kb ladder, 1-20- picked colonies of the putative pHS1 plasmid (figure 22, left plate), 21-22 – picked colonies of negative control, vector only (figure 22, right plate), 23-24- picked colonies of the negative control, pCasSA plasmid commercially available within *E. coli* (refer to figure 15), 25-26- positive control, purified assembled arm products.

3.2.6. Confirmation of the repair arms within the pHS1 plasmid

DNA sequencing results of the pHS1 plasmid with primer A (figure 24) (Appendix B) aligned with the JB wild-type sequenced genome repair arms using BlastN sequence analysis, confirming the presence of the repair arms within the pHS1 plasmid (figure 24).
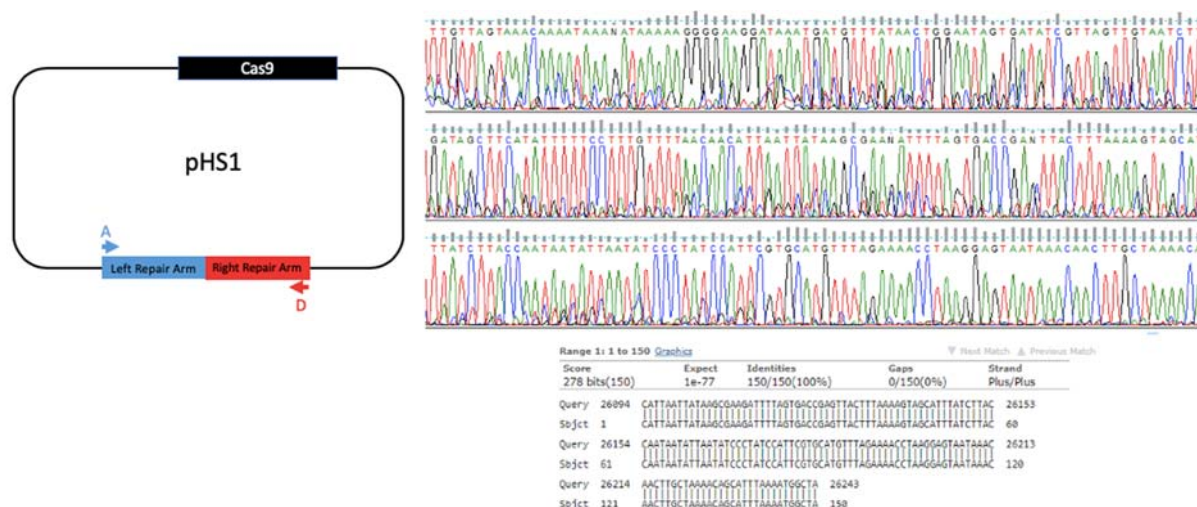
Figure 24. DNA Sequencing results of pHS1.
DNA sequencing results of the pHS1 plasmid from primer A.

3.2.7. DNA sequencing of the pHS1 plasmid as a negative control for gRNA

As expected, DNA sequencing of the purified pHS1 plasmid did not produce a DNA

sequence from primer F (figure 25) confirming the absence of the gRNA sequences within the

pHS1 plasmid.
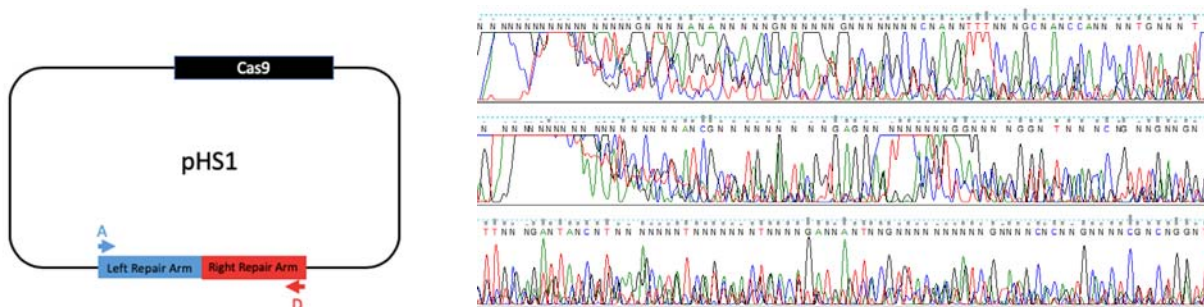
Figure 25. DNA Sequencing of pHS1.
DNA Sequencing results of the pHS1 plasmid with Primer F.

3.3. Construction of the pHS3 plasmid

3.3.1. Transforming *E. coli* with the pHS3 plasmid and screening

Following Golden Gate assembly of the gRNA into the pHS1 plasmid (pHS3), the

plasmid was transformed into *E. coli* via heat-shock. Isolated colonies that putatively contained

the pHS3 plasmid were observed after overnight growth on an LB plate containing 50 µg/mL of

kanamycin and no colonies were visualized on a negative control Golden Gate Assembly

reaction of linearized pHS1 plasmid without a gRNA insert (figure 26).
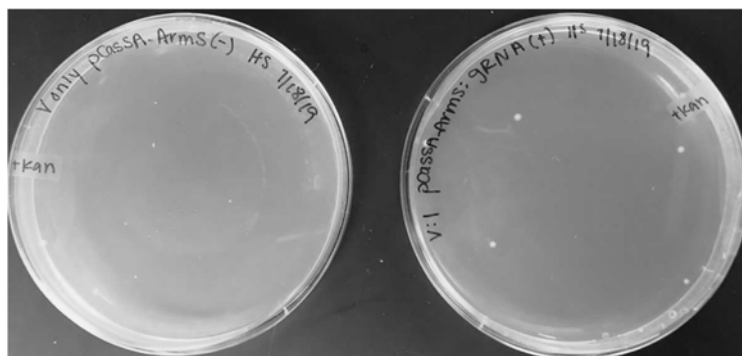
Figure 26. Image of *E. coli* containing the pHS3 plasmid.
Left plate- The negative control plate of vector only (pHS1) without gRNA insert yielded no colonies.
Right plate-Isolated colonies were observed on the LB plate containing the transformed cells with the pHS3 plasmid.

Three colonies from the right plate were screened by PCR using primers E and F to

confirm the presence of the gRNA within the pHS3 plasmid yielded bands of the expected size

of 500 bp (figure 27).

Figure 27. Gel Electrophoresis Image of Polymerase Chain Reactions to Screen for gRNA within the pHS3 plasmid.
L- 1 kb NEB ladder, 1- pHS3 sample #1 (expected size = 500 bp), 2- pHS3 sample #2 (expected size = 500 bp), 3- pHS3 sample #3 (expected size =500 bp), 4- pHS1 (negative control), 5- pCasSA (negative control), 6- water (negative control).

3.3.2. Confirmation of the repair arms and gRNA within the pHS3 plasmid

DNA sequencing results of the pHS3 plasmid with primers A (Appendix B) aligned with the JB wild-type sequenced genome repair arms using BlastN sequence analysis confirming the presence of the repair arms within the pHS3 plasmid (figure 28).
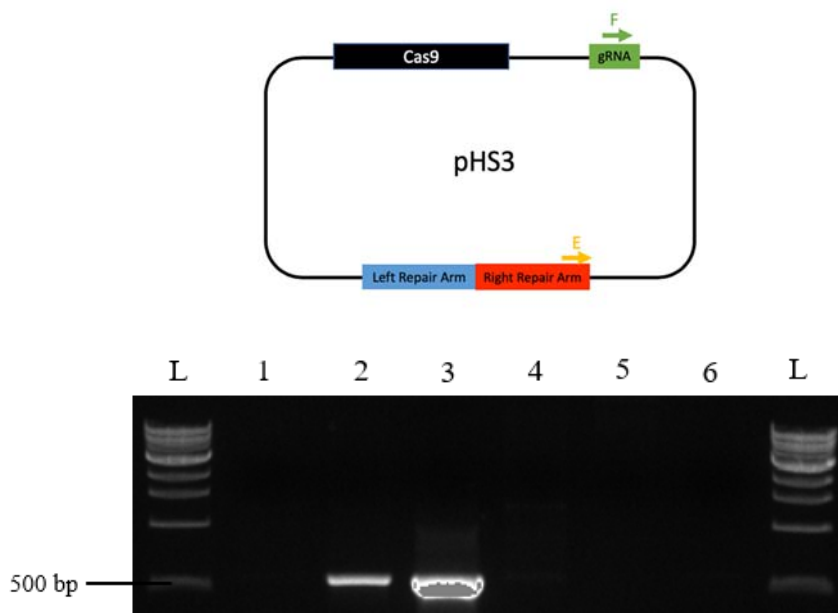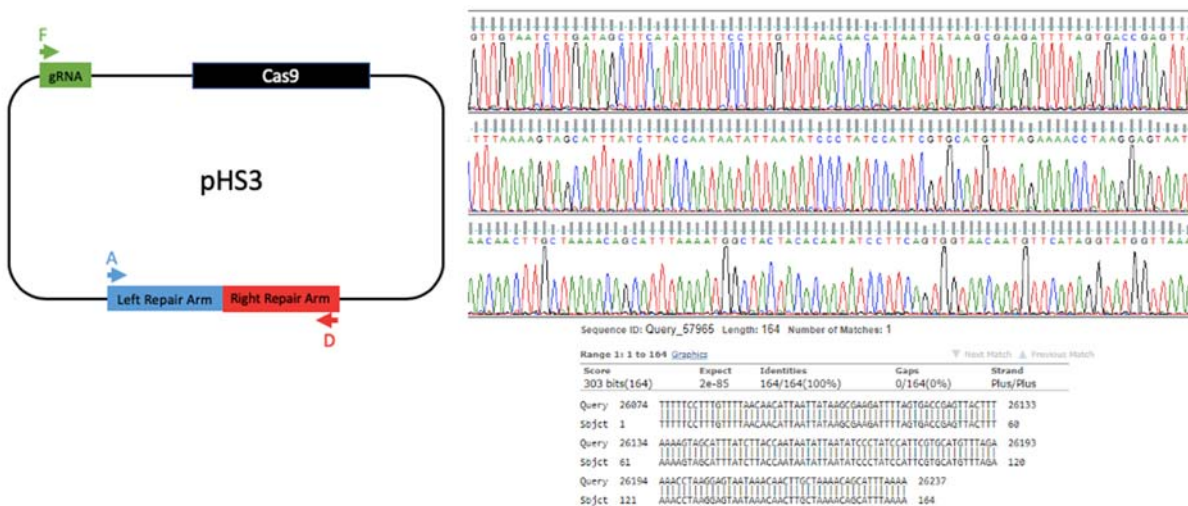

Figure 28. DNA Sequencing of pHS3.
DNA Sequencing of the pHS3 plasmid with primer A.

DNA sequencing results of the pHS3 plasmid with primer F (Appendix B) aligned with the JB wild-type sequenced genome repair arms using BlastN sequence analysis confirming the presence of the gRNA within the pHS3 plasmid (figure 29).
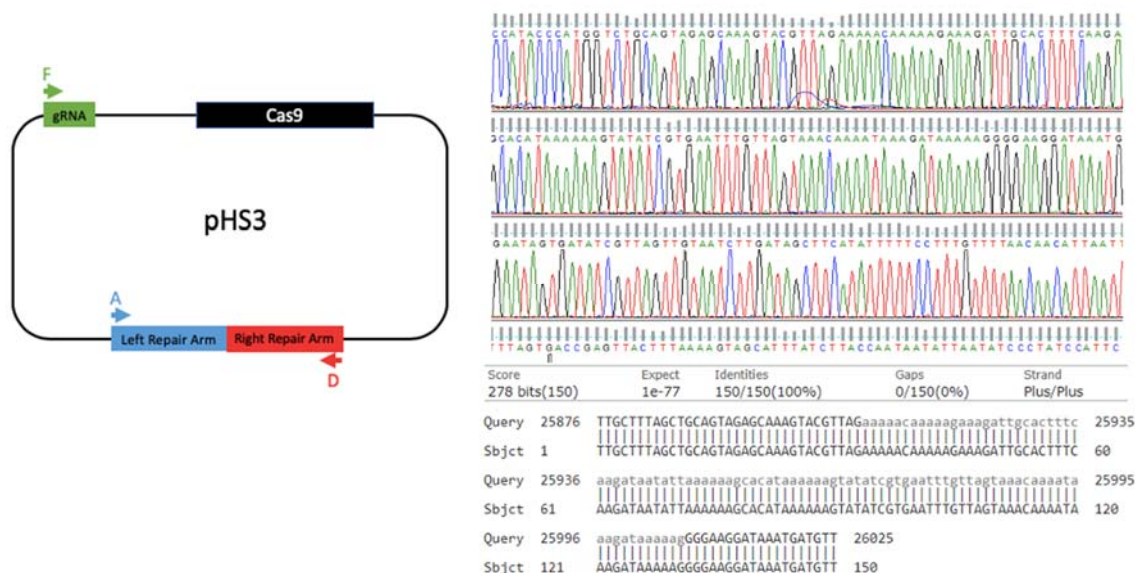
Figure 29. DNA Sequencing of pHS3.
DNA Sequencing results of the pHS3 plasmid with primer F.

3.4. Insertion of the pHS3 plasmid into *S. aureus* RN4220

3.4.1. Transforming pHS3 into *S. aureus* RN4220 and screening.

S. aureus RN4220 transformed with the pHS3 plasmid yielded isolated colonies that

putatively contained pHS3 on a TSA (supplemented with 25 % dextrose and 0.1 M CaCl$_2$) plate

with 10 µg/mL of chloramphenicol. No colonies were observed on a TSA (supplemented with 25

% dextrose and 0.1 M CaCl$_2$) plate with 10 µg/mL of chloramphenicol of wild-type *S. aureus*

RN4220 (negative control) (figure 30).
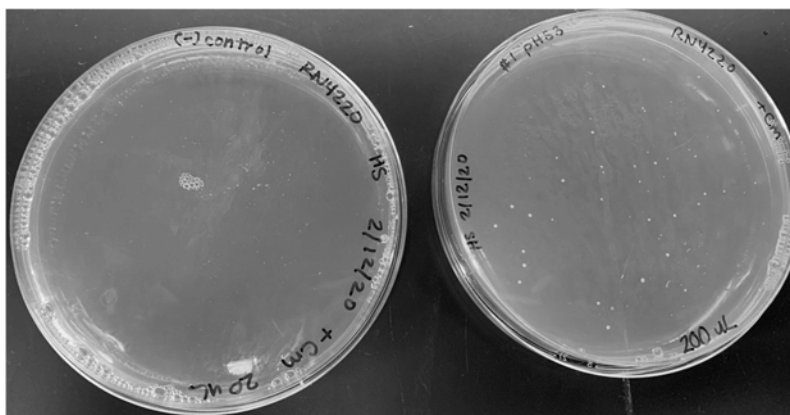
Figure 30. Image of TSA plates (10 µg/mL chloramphenicol) containing isolated *S. aureus* RN4220 colonies containing the pHS3 plasmid.

Left plate- No colonies were observed on the negative control plate of *S. aureus* RN4220.
Right plate- Isolated colonies of *S. aureus* RN4220 putatively containing the pHS3 plasmid were observed.

Polymerase chain reactions to screen for the presence of the pHS3 plasmid using primers A and D within the *S. aureus* RN4220 colonies yielded bands of the expected size (1,877 bp) on gel electrophoresis for at least 8/20 selected colonies indicating the presence of the pHS3 plasmid within *S. aureus* RN4220 (figure 31, lanes 1, 2, 3, 11, 13, 14, 18 and 20).

Figure 31. Gel Electrophoresis Image of Polymerase Chain Reactions to Screen for the presence of pHS3 within *S. aureus* RN4220.
GeneRuler 1 kb Plus DNA Ladder, 1-20 picked colonies after electroporation of pHS3 into *S. aureus* RN4220 (expected size = 1,877), 21- purified pHS3 plasmid, positive control (expected size= 1,877), 22- picked colony of *S. aureus* RN4220, negative control, 23- water, negative control. *- positive PCR amplicon.
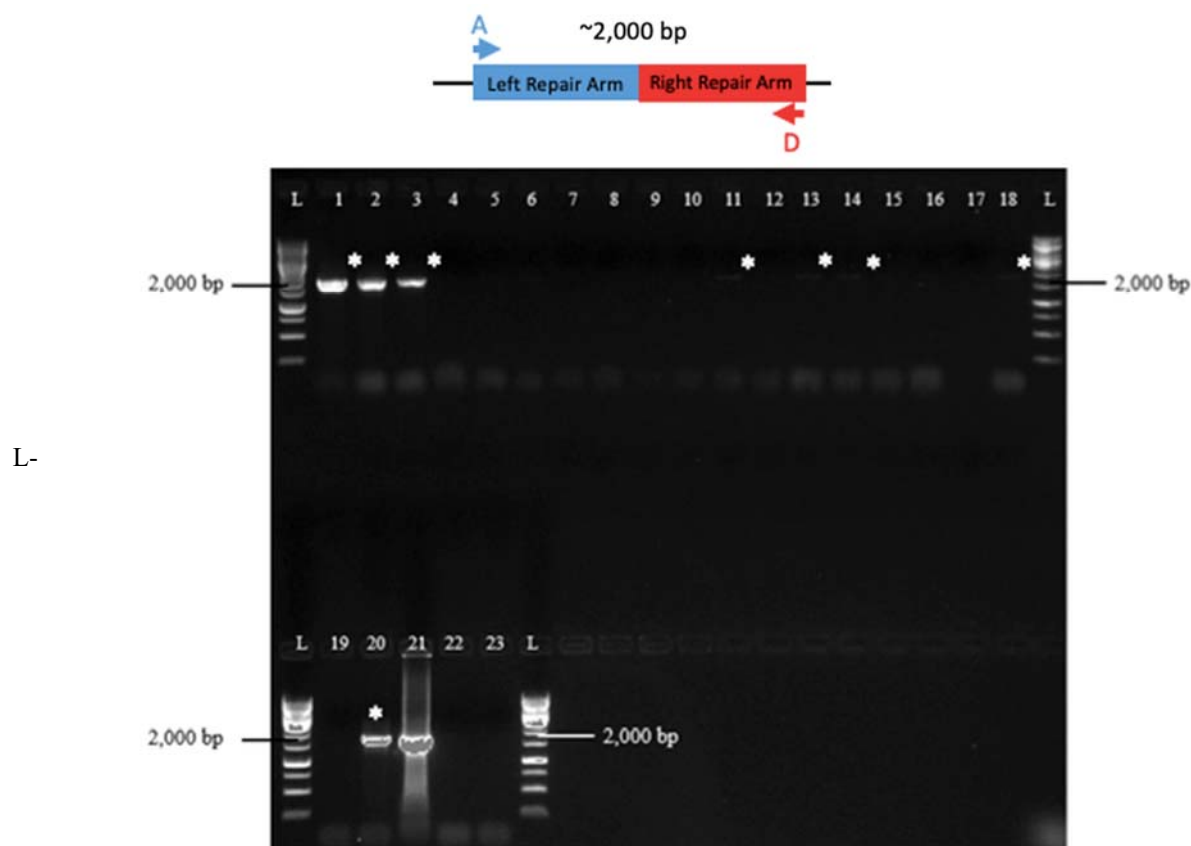
3.5. Infection of *S. aureus* RN4220-pHS3 with bacteriophage JB

3.5.1. Liquid Infection of *S. aureus* RN4220-pHS3 with bacteriophage JB

Liquid culture infection (10 uL) of JB in *S. aureus* RN4220-pHS3 and *S. aureus* RN4220 were observed after the two-day incubation period. The *S. aureus* RN4220-pHS3 cultures after JB liquid infection appeared clear and after centrifugation (2,000 rpm for 5 minutes) no bacterial pellet was observed (figure 27). The absence of bacterial growth from *S. aureus* RN4220-pHS3 culture after JB liquid infection suggested the presence of deletion mutant JB (JBΔ30-33) with strictly lytic capabilities. The *S. aureus* RN4220 culture after JB liquid infection appeared cloudy

and after centrifugation (2,000 rpm for 5 minutes) a bacterial pellet was observed (figure 32).

The presence of bacterial growth from *S. aureus* RN4220 culture after JB liquid infection

suggests the formation of lysogens, which was expected due to wild-type JB's lysogenic

capabilities.

Figure 32. Liquid infection of JB in *S. aureus* RN4220-pHS3 and *S. aureus* RN4220.
The image shows the difference in bacterial growth after JB infection of *S. aureus* RN4220 (left culture) compared to *S. aureus* RN4220-pHS3 (right culture).

3.5.2. Plaque assay of *S. aureus* ATCC 33742 (PS88) with bacteriophage JB and putative deletion mutant JBΔ30-33.

After incubation, the resultant plaques from wild-type JB on *S. aureus* ATCC 33742

(PS88) appeared small and turbid/cloudy, which is indicative of a temperate bacteriophage. In

contrast, the resultant plaques from lysate of putative deletion mutant JBΔ30-33 on *S. aureus*

ATCC 33742 (PS88) appeared small and clear, which is indicative of a lytic bacteriophage

(figure 33), suggesting deletion of genes 30-33 and JB's ability to form lysogens.
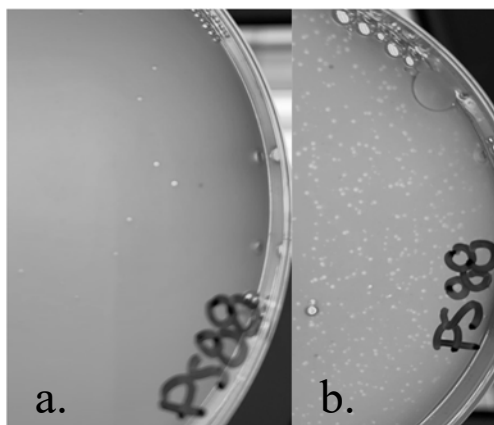
Figure 33. Plaque assay infections on *S. aureus* ATCC 33742 (PS88).

a.) Resultant plaques from putative deletion mutant JBΔ30-33. b.) Resultant plaques from wild-type JB.

3.1. Confirmation of deletion mutant JBΔ30-33

3.1.1. Screening plaques for deletion mutant JBΔ30-33 by PCR

Polymerase chain reactions were used to screen for the presence or absence of genes 30-33 within the JB phage genome yielded the expected results (figure 34). The plaque from the putative deletion mutant JBΔ30-33 yielded a band of approximately 2,000 bp, indicating the deletion of genes 30-33 (figure 34). Plaques from the wild-type JB phage yielded a band of approximately 5,000 bp, indicating the presence of genes 30-33 (figure 34). The purified pHS3 as a positive control plasmid yielded a band of approximately 2,000 bp (figure 34). The negative controls of an isolated colony from *S. aureus* ATCC 33742 (PS88) and sterile nuclease-free water yielded no bands (figure 34).
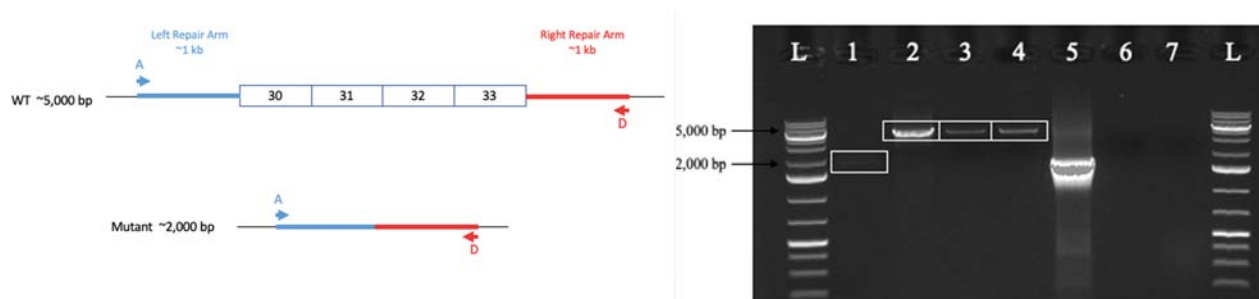
Figure 34. Gel electrophoresis image of Polymerase Chain Reactions to screen for the presence or absence of genes 30-33 in phage plaques.

L-GeneRuler 1 kb Plus DNA Ladder, 1- putative deletion mutant JBΔ30-33 plaque, 2-4 wildtype JB plaque, 5- pHS3 purified plasmid, 6-PS88 colony, 7- water.

3.1.2. DNA sequencing of PCR product from wild-type JB and JBΔ30-33.

DNA sequencing results of wildtype JB (5,000 bp) product with primer A (Appendix B) aligned with the JB wildtype sequenced genome using BlastN sequence analysis (figure 35).

Figure 35. DNA sequencing results of wildtype JB (5,000 bp) PCR product.
DNA sequencing of the wildtype JB (5,000 bp) PCR product from primer A aligned with the full genome JB sequence using BlastN sequence analysis.

DNA sequencing results of wildtype JB (5,000 bp) product with primer F (Appendix B) aligned with the JB wildtype sequenced genome using BlastN sequence analysis (figure 36).
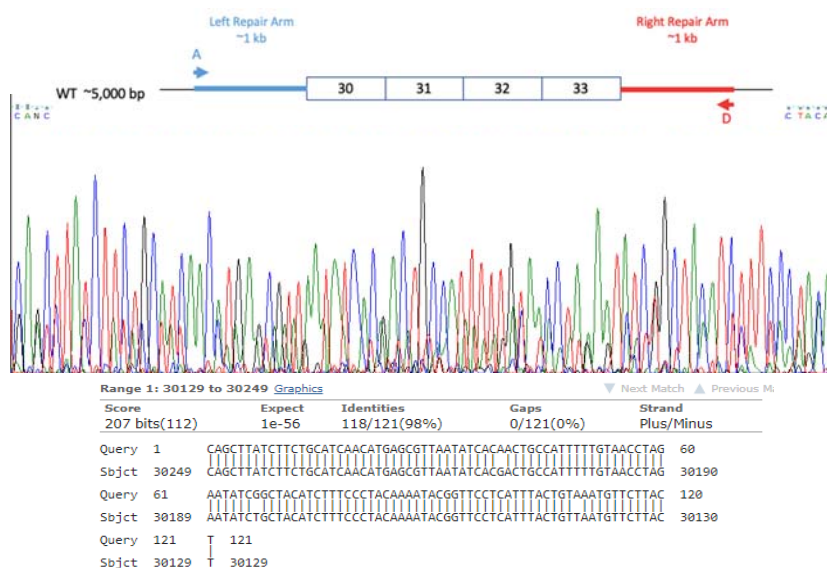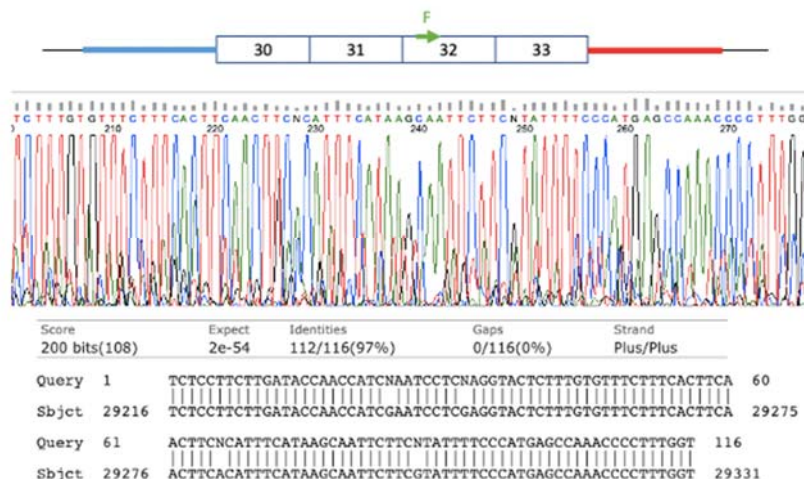
Figure 36. DNA sequencing results of wildtype JB (5,000 bp) PCR product.
DNA sequencing of the wildtype JB (5,000 bp) PCR product from primer F aligned with the full genome JB sequence using BlastN sequence analysis.

DNA sequencing results of deletion mutant JBΔ30-33 product with primer A (Appendix B) aligned with the JB wildtype sequenced genome using BlastN sequence analysis confirming the presence of the repair arms (figure 37).

Figure 37. DNA sequencing results of JBΔ30-33 (2,000 bp) PCR product.
DNA sequencing of the JBΔ30-33 (2,000 bp) PCR product aligned with the full genome JB sequence using BlastN sequence analysis.

DNA sequencing results of deletion mutant JBΔ30-33 product with primer F (Appendix B) did

not produce a DNA sequence confirming the absence of genes 30-33 (figure 38).

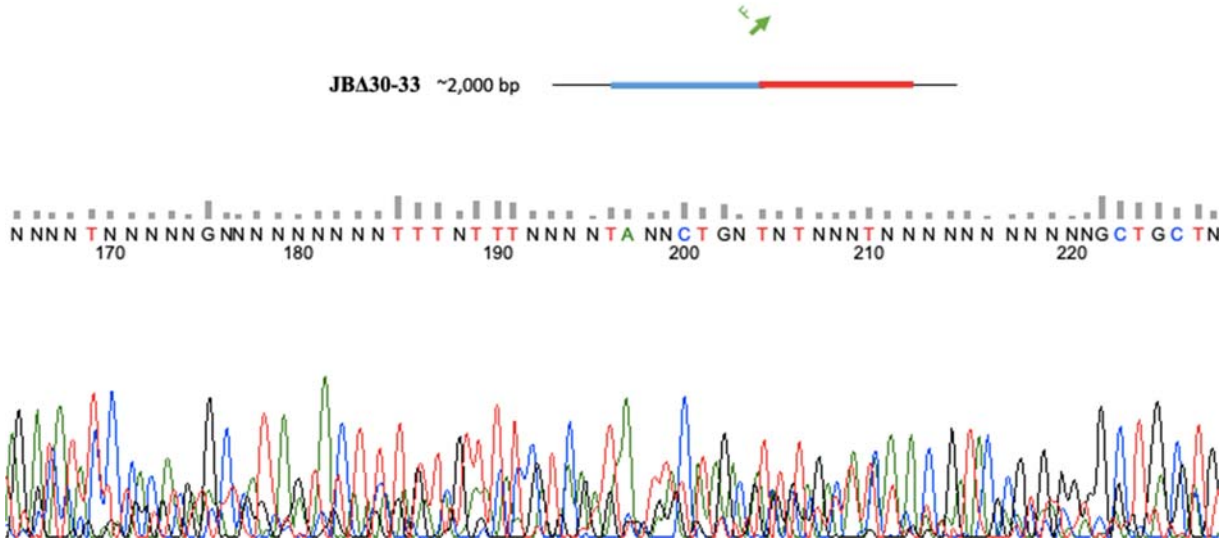**Figure 38. DNA sequencing results of JBΔ30-33 (2,000 bp) PCR product.**
DNA sequencing of the JBΔ30-33 (2,000 bp) PCR product did not produce a DNA sequence.

4. Conclusion

Staphylococcal bacteriophage JB, isolated from dairy cow hair samples, has the ability to infect methicillin-resistant *Staphylococcus aureus* (MRSA). After genome annotation, bacteriophage JB was determined to be a temperate phage that contains putative toxin and integrase genes. In order to use JB as a potential phage for mammalian organisms, deletion of the toxin and integrase coding genes is essential to produce a safe strictly lytic phage.

This study used a commercially available CRISPR/Cas9 expression plasmid, pCasSA, to generate the pHS3 plasmid. The pHS3 plasmid contains a gRNA, a sequence specific to a cut site within the genes of interest upstream of a PAM sequence to guide the Cas enzyme to the genes 30-33 within the JB genome. The pHS3 plasmid also contained 1,000 bp sequences flanking the genes of interest (repair arms) to mediate homologous recombination after the Cas enzyme's double-stranded break of the JB genome, effectively removing genes the toxin and integrase genes. The creation of the pHS3 plasmid with the repair arms and gRNA was confirmed by PCR and DNA Sequencing.

Transformation of the pHS3 plasmid into *S. aureus* RN4220 generated *S. aureus* RN4220-pHS3 which was subsequently infected with the JB bacteriophage. Liquid infection of JB in *S. aureus* RN4220-pHS3 generated the deletion mutant JBΔ30-33. Plaque assays of JBΔ30-33 on *S. aureus* PS88 showed a clear plaque morphology indicating a lytic bacteriophage, in contrast to wildtype JB turbid plaque morphology indicating a temperate bacteriophage. The creation of deletion mutant JBΔ30-33 was confirmed by PCR and DNA Sequencing.

The genetically engineered derivative of JB phage, JBΔ30-33, had the problematic integrase and toxin genes removed for safety and demonstrated lytic capabilities in liquid infections and plaque assays. Further characterization of JBΔ30-33 is necessary to determine if

JBΔ30-33 host range on clinical isolate strains of *S. aureus* has altered infectivity compared to wildtype JB. Future studies of JBΔ30-33 and wildtype JB can be performed *in vitro* on cell cultures and *in vivo* on murine organisms infected with *S. aureus* to determine its safety and efficacy in phage therapy. Further characterization of JBΔ30-33 can be performed by imaging JBΔ30-33 by transmission electron microscopy.

References Cited

1. Wommack, K.E. & Colwell, R.R. (2000). Virioplankton: viruses in aquatic ecosystems. Microbiol Mol Biol Rev, 64(1), 69-114. doi: PMC98987.

2. Twort, F. (1915). An investigation on the nature of ultra-microscopic viruses. *The Lancet,* 1(3)127-129.

3. d'Herelle, F. (1917). Sur un microbe invisible antagoniste des bacillus dysenterique. *Acad Sci Paris,* 159, 373-5.

4. Bacteriophage—An overview | sciencedirect topics. (n.d.). Retrieved August 6, 2019, from https://www.sciencedirect.com/topics/medicine-and-dentistry/bacteriophage\

5. Hatfull, G. & Hendrix, R. (2011). Bacteriophages and their genomes. *Current Opinion in Virology*, 1, 298-303. doi: 10.1016/j.coviro.2011.06.009.

6. Fokine, A. & Rossmann, M. (2014). Molecular architecture of tailed double-stranded DNA phages. *Bacteriophage,* 4, e28281. doi: 10.4161/bact.28281

7. Hatfull, et. al., (2006). Exploring the mycobacteriophage metaproteome: Phage genomics as an educational platform. *PLoS Genet.,* e92. doi: 10.1371/journal.pgen.0020092.

8. Khan Academy (2018). Viruses: Bacteriophages: Bacteria-infecting viruses. The lytic and lysogenic cycles. Retrieved from https://www.khanacademy.org/science/biology/biology-of-viruses/virus-biology/a/bacteriophages

9. Groth, A., & Calos, P. (2004). Phage integrases: Biology and applications. *J. Mol. Biol.,* 335, 667-678. doi: 10/1016/j.jmb/2003.09.082.

10. Lewis, J., & Hatfull, G. (2001). Control of directionality in integrase-mediated recombination: examination of recombination directionality factors (RDFs) including Xis and Cox proteins. *Nucleic Acids Res.* 29(11), 2205-2216. doi: 10.1093/nar/29.11.2205.

11. Centers for Disease Control and Prevention (CDC). (2019). *Antibiotic/ Antimicrobial Resistance (AR/AMR).* Retrieved from https://www.cdc.gov/drugresistance/about.html

12. Fleming, A. (1945). *Penicillin.* Nobel Lecture. Retrieved from https://www.nobelprize.org/uploads/2018/06/fleming-lecture.pdf

13. Centers for Disease Control and Prevention (CDC). (2019). *Biggest threats and data.* Retrieved from https://www.cdc.gov/drugresistance/biggest-threats.html.

14. Davies, J. & Davies, D. (2010). Origins and Evolution of Antibiotic Resistance. *Microbiol Mol Biol Rev,* 74(3), 417-433. doi: 10.1128/mmbr.0016-10.

15. Lin, D., Koskell, B., & Lin, H. (2017). Phage therapy: An alternative to antibiotics in the age of multi-drug resistance. *World J Gastrointest Pharmacol Ther,* 8(3), 162-173. doi: 10.4292/wjgpt.v8.i3.162.

16. Altamirano, F. & Barr, J. (2019). Phage therapy in the postantibiotic era. *Clin Microbiol Rev,* 32 (2), 1-25. doi: 10.1128/CMR.00066-18.

17. Schooley, R., *et. al.* (2017). Development and use of personalized bacteriophage-based therapeutic cocktails to treat a patient with a disseminated resistant *Acinetobacter baumannii* infection. *Antimicrob Agents Chemother,* 61 (10), e00954-17. doi:10.1128AAC.00954-17.

18. Dedrick, R., Guerrero-Bustamante, C., Garlena, R., Russell, D., Ford, K., Harris, K., Gilmour, K., Soothill, J., Jacobs-Sera, D., Schooley, R., Hatfull, G., & Spencer, H. (2019). Engineered bacteriophages for treatment of a patient with a disseminated drug-resistant *Mycobacterium abscessus. Nature Medicine*, 25, 730-733. doi: 10.1038/s41591-019-0437-z

19. Hassoun, A., Linden, P., & Friedman, B. (2017). Incidence, prevalence, and management of MRSA bacteremia across patient populations- a review of recent developments in MRSA management and development. *Critical Care,* 21, 211. doi: 10.11.s13054-017-1801-3.

20. Centers for Disease Control and Prevention (CDC). *Deadly Staph infections still threaten the U.S.* Retrieved from https://www.cdc.gov/media/releases/2019/p0305-deadly-staph-infections.html

21. Gregory, J. (2017). Doped apatite nanoparticles: Characterization and biomedical relevance. *Dissertation: Doctor of Philosophy in Interdisciplinary Studies, Biomedical Engineering.* The University of Montana.

22. Oliver, A., & Gersbach, C. (2019) The next generation of CRISPR-Cas technologis and applications. *Nature Reviews Molecular Cell Biology,* 20, 490-507. doi: 10.1038/s41580-019-0131-5.

23. Jinek, M., Chylinski, K., Fonfara, I., Hauer, M., Doudna, J., & Charpentier, E. (2012). A programmable dual RNA-guided DNA endonuclease in adaptive bacterial immunity. *Science,* 337(6096), 816-821. doi: 10.1126/science.1225829.

24. Aslan, A. (2018) Phage Genetic Engineering using CRISPR-Cas systems. *Viruses,* 10, 335. doi: 10.3390/v10060335.

25. Chen, W., Zhang, Y., Yeo, W.S., Bae T., & Quanjiang J. (2017). Rapid and efficient

genome editing in *Staphylococcus aureus* by using an engineered CRISPR/Cas9

System. *Journal of the American Chemical Society,* 139(10*),* 3790-3795.

doi:10.1021/jacs.6b13317.

5. Appendix A: Repair Arms and gRNA isolated from the JB genome.

Left Repair Arm:

5'CTGCAGTAGAGCAAAGTACGTTAGAAAAACAAAAAGAAAGATTGCACTTTCAAGA

TAATATTAAAAAAGCACATAAAAAAGTATATCGTGAATTTGTTAGTAAACAAAATA

AAGATAAAAAGGGGAAGGATAAATGATGTTTATAACTGGAATAGTGATATCGTTAG

TTGTAATCTTGATAGCTTCATATTTTTCCTTTGTTTTAACAACATTAATTATAAGCGA

AGATTTTAGTGACCGAGTTACTTTAAAAGTAGCATTTATCTTACCAATAATATTAAT

ATCCCTATCCATTCGTGCATGTTTAGAAAACCTAAGGAGTAATAAACAACTTGCTAA

AACAGCATTTAAAATGGCTACTACACAATATCCTTCAGTGGTAACAATGTTCATAGG

TATGGTTAAAGACCATCAAGCACAAGTCCACTGTTTTGGTGAATCTACCTATACCTA

TAACCAAAATAAAGAAAACCTAATATTAAAAAAAGACATAAATAAGTCATGGTTAA

ATTCATTAAAGAATTTGAAGTCACTTATTAAATCAGAAGGATTTAAAAAGAATTTTT

TAAATAACTTAGCTGAAGCTTAAGTTCTCGTATTACCTTCGATGATTATGAATTTTGC

TCAGCATGTAAAACCACACCACCTATTAATTTAGGAGTGTGGTTATTTTAATATATG

AAGCTAAAATAACTACAAATGATACCATTTTTGATACCATTTTGTTGTAAAACAGAA

AAAATAAGGAAAATAAAAAAGGCAAAAAAACGCATTAAATCAACGTTTATTGTCTC

ATGAAATTTAAATGTATATAAATTTCACTTCCCATGGGTCATTATGAATTCTTATTTT

AGGCTTGTTATTAC 3'

Right Repair Arm:

5'GTTTACTTTATGTGTTGACACTTTACTTTTAGTGTAGTAAATTAGATGCATACCTTA

CAAGGAGGTGACAACATGACAGATACAATTGAGGCATTTTCTCTAAAGGGTGCGCG

AAATGAATTTGATTACACGCAAGAGCAAATAGCTGATAAATTAGGGGTTTCTCGAG

CACAGTATATTGCGTGGGAAAAAGGTGATGTAATACCTAAAAGCATGGTAGTTTAT

GCTTTAGCTTACATCTATGGTATTAACGCTGACTTATTAAGAGTCAGCAAAAAATT

TAAAACTAACTTCACTTAAAGTGAAGTTGTGTAAAAACACGACAAAGAAAACAA

ACTATTTAAAAGGAGGAACTCAGATGCAAGCATTACAAACATTTAATTTTGAAGAAT

TACCAGTAAGAACATTAACAGTAAATGAGGAACCGTATTTTGTAGGGAAAGATGTA

GCAGATATTCTAGGTTACAAAAATGGCAGTCGTGATATTAACGCTCATGTTGATGCA

GAAGATAAGCTGACGTACCAAATCAGTACCGCAGGTCAAAGACGAAATCAAACAAT

CATCAACGAATCGGGTTTATACAGCCTAATCTTCTCATCAAAACTAGAATCAGCTAA

ACGATTCAAACGTTGGGTAACTTCAGACGTCCTACCCGCTATTCGAAAACACGGTAT

CTACGCAACAGACAATGTAATTGAACAAACATTAAAAGATCCAGACTACATCATTA

CAGTGTTGACTGAGTATAAGAAGAAAAAGAGCAAAACTTACTTTTACAACAAGAA

ATTGGAGAGCTAAAACCCAAAGCAGACTATGTAGATGAAATCTTAAAGTCAACTGG

AACATTAGCTACAACTCAAATCGCGGCAGACTACGGTATATCAGCACAAAAGTTAA

ACAAACTACTACACGAAGCTAGATTACAACGAAAGTGAATAAACAGT 3'

gRNA:

5' CAAAGCTTCTACAATTTCGCGTAA<u>TGG</u> 3'

      3'CGAAGATGTTAAAGCGCATTACCGAAA 5'

*underlined PAM sequence

6. Appendix B: Primers

6.1. Table I

Primer Name	Primer Sequence (5'to 3')	Melting Temperature (T$_m$)	G/C Content
A (Left Repair Arm Forward)	GATCTGTCCATACCCATGG TCTGCAGTAGAGCAAAGT AC	64.8ºC	48.7 %
B (Left Repair Arm Reverse)	TGTCAACACATAAAGTAA ACGTAATAACAAGCCTAA AATAAGAATTCATAATGA CC	62.5ºC	62.5 %
C (Right Repair Arm Forward)	GTTTACTTTATGTGTTGAC AC TTTACTTTTAGTG	55.4ºC	29.4 %
D (Right Repair Arm Reverse)	AAGATACAGGTATATTTTT CTGACTGTTTATTCACTTT TCGTTGTAATC	60.7ºC	28.6 %
E (Confirm guide)	GATTCACCAAAACAGTGG ACT	54.5ºC	42.9 %
F (Forward gRNA)	CAAAGCTTCTACAATTTCG CGTAATGG	53.9ºC	43.5 %

G (Reverse gRNA)	CGAAGATGTTAAAGCGCA TTACCGAAA	54.1ºC	43.5 %
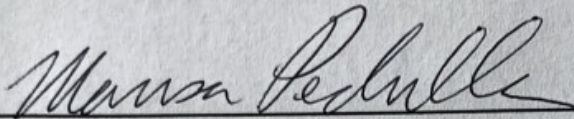
*underlined sequences are homologous to pCasSA cloning sites
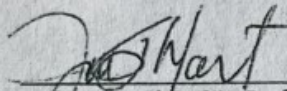
7. Appendix C: Media

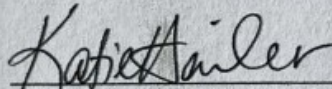|	
Tryptic Soy Broth ++ (TSB ++)	To 1 L of sterile ddH$_2$0, 30 g Tryptic Soy Broth (Sigma-Aldrich) were added. The solution was stirred until fully dissolved and heated until it came to a boil. The solution was autoclaved on a liquid cycle for 20 minutes. Prior to use, 25 mL/L of a 25 % sterile solution of dextrose and 10mL/L of a sterile 0.1 M CaCl$_2$ solution was added. TSB ++ was stored in 4°C.
Tryptic Soy Agar ++ (TSA ++)	To 1 L of sterile ddH$_2$0, 40 g Tryptic Soy Agar (Sigma-Aldrich) were added. The solution was stirred until fully dissolved and heated until it came to a boil. The solution was autoclaved on a liquid cycle for 20 minutes. Once the solution was cool to the touch, 25 mL/L of a 25 % sterile solution of dextrose and 10mL/L of a 0.1 M CaCl$_2$ sterile solution were added. The mixture was poured directly into Petri dishes and stored in 4°C or stored in a sterile container at room temperature.
Top Agar ++ (TSTA++)	A 1:1 solution of TSA++: TSB++ is combined and the mixture is kept molten at 65°C or stored at room temperature.
CaCl$_2$ (0.1 M)	1.47 g of Calcium chloride was added to 100 mL of ddH$_2$0 and stirred until fully dissolved. The solution was autoclaved on a liquid cycle for 20 minutes.

SIGNATURE PAGE

This is to certify that the thesis prepared by Hannah Sparks entitled "Genetic removal of toxin and integrase genes from a staphylococcal bacteriophage" has been examined and approved for acceptance by the Department of Industrial Hygiene and Biological Sciences, Montana Technological University, on this 24th day of April, 2020.
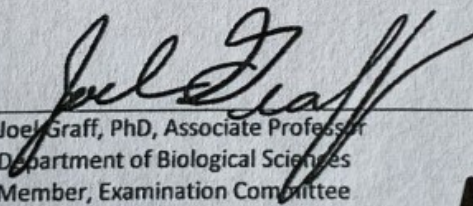
Marisa Pedulla, PhD, Professor
Department of Biological Sciences
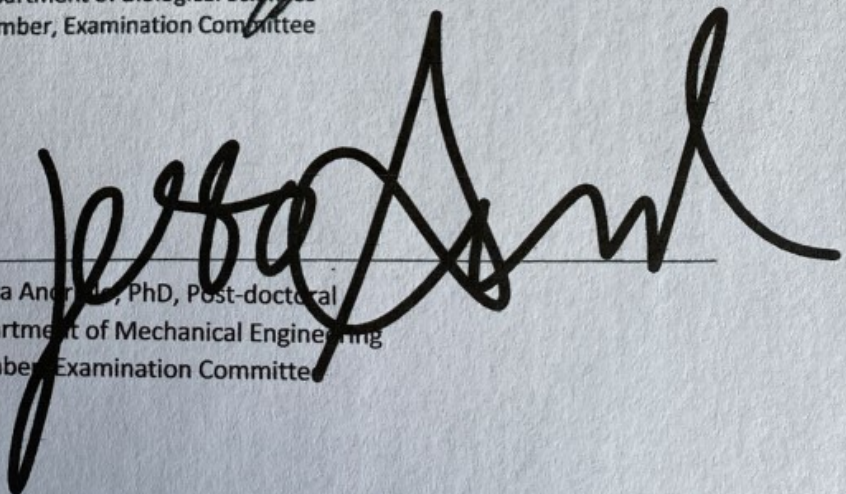Chair, Examination Committee

Julie Hart, PhD, CIH, Professor and Department Head
Department of Safety, Health and Industrial Hygiene
Member, Examination Committee

Katie Hailer, PhD, Associate Professor and Department Head
Department of Chemistry and Geochemistry
Member, Examination Committee

Joel Graff, PhD, Associate Professor
Department of Biological Sciences
Member, Examination Committee

Jessica Andriolo, PhD, Post-doctoral
Department of Mechanical Engineering
Member, Examination Committee